Academia
Molecular Biology and Genomics

10.20935/AcadMolBioGen8651

Review Article

TBXT expression in development and cancer: signaling, enhancers and epigenetics

Akechai Kongprajug[1,2,3], Mohammad Hamza[1], Fiona C. Wardle[1,*]

[1] Randall Centre for Cell and Molecular Biophysics, King's College London, London, UK
[2] Project Development for Research Excellence Division, Bureau for Research and Innovation Management, Chulabhorn Royal Academy, Bangkok, Thailand
[3] Center for Cancer Discovery and Genomics, Chulabhorn Royal Academy, Bangkok, Thailand
* Correspondence: fiona.wardle@kcl.ac.uk

Received: 28 July 2026 | **Accepted:** 12 November 2026 | **Published:** 19 November 2026

Abstract

The transcription factor TBXT plays a pivotal role in vertebrate embryogenesis and has emerged as a key regulator in some cancers. During embryonic development, TBXT governs notochord differentiation and posterior body elongation, with its expression tightly controlled by signaling pathways including Nodal/Activin, bone morphogenetic protein (BMP), fibroblast growth factor (FGF), WNT, and retinoic acid (RA). These pathways act through conserved and species-specific cis-regulatory elements (CREs) that integrate activating and repressive inputs to ensure precise spatiotemporal expression. Beyond development, *TBXT* is aberrantly expressed in multiple cancers and functions in a context-dependent manner, acting as a driver in chordoma and promoting metastasis and poor prognosis in epithelial cancers such as triple-negative breast and non-small cell lung cancer, while exerting a protective role in glioma. Its dysregulation is influenced by signaling pathways including FGF, phosphoinositide 3-kinase (PI3K)/protein kinase B (AKT), transforming growth factor β (TGF-β), WNT, and hypoxia, and by epigenetic mechanisms. Notably, a super-enhancer downstream of *TBXT* drives its expression in chordoma, but the specific CREs that drive expression in other cancers remain uncharacterized. Elucidating how signaling pathways and CREs interact to regulate *TBXT* expression may offer avenues for targeted therapeutic interventions in cancers dependent on TBXT.

Keywords: *TBXT*; enhancer; gene regulation; signaling

1. Introduction

TBXT, also known as T or Brachyury, is the founding member of the T-box family of transcription factors, which are characterized by a highly conserved DNA-binding domain. The mouse *Brachyury* mutation, identified in an X-ray-induced mutagenesis screen, was first described by Nadine Dobrovolskaya-Zavadskaya in 1927 [1]. Mice heterozygous for the mutation have a short tail, while the homozygous mutation is lethal in utero, due to abnormalities in development of extra-embryonic structures. These mice also lack a differentiated notochord and caudal structures, including somites. The gene was subsequently cloned from mouse and from many other organisms, and is now well studied in embryonic development [1]. In the past two decades, however, it has also

become clear that TBXT plays a role in various human cancers, where up- and downregulation of its expression can lead to tumor growth, metastasis, and/or resistance to radio- and chemotherapy [2]. Several recent reviews have summarized the roles of *TBXT* in cancer [2–5]. Others have focused on its function in vertebrate embryonic development and evolution [1, 6, 7]. However, these reviews mainly address what *TBXT* does in development and cancer, and how the protein can be targeted for therapies, rather than how its expression is controlled, and to our knowledge the mechanisms regulating *TBXT* expression in the embryo and in cancer have not previously been considered together. Here we compare our current understanding of how *TBXT* expression is regulated during vertebrate embryonic development and in cancer, after briefly reviewing its function. We review the evidence for different signaling pathways regulating *TBXT* expression directly or indirectly, and discuss the cis-regulatory elements (CREs) and chromatin landscape that mediate this signaling. This comparison highlights a large gap in our understanding of how *TBXT* is regulated at a transcriptional level in cancer, where very few studies have addressed direct transcriptional regulation through signaling and CREs.

A note on gene nomenclature. When referring to a gene or protein in a particular animal model or in humans we use the gene/protein nomenclature convention for that species (i.e., *tbxt*/Tbxt for *Xenopus* and zebrafish, *Tbxt*/TBXT for mouse, and *TBXT*/TBXT for human). When referring to a gene/protein in a general sense or in more than one species that have different nomenclature rules, we use the human nomenclature convention.

2. The role of *TBXT* in vertebrate development and cancer

Since its discovery as a gene required for tail outgrowth and notochord development in mouse, a conserved role for *TBXT* has been shown in other vertebrates [6]. For instance, zebrafish *no tail* mutant embryos, which have a *tbxta* loss-of-function mutation, lack a notochord and posterior structures. This no notochord/*no tail* phenotype is consistent with the expression pattern of *TBXT* during development. Initially *TBXT* is expressed in the primitive streak in amniotes, and in more basal vertebrates in the marginal zone cells that will move through the blastopore [6]. As cells migrate through the primitive streak or blastopore they downregulate *TBXT* expression except in axial cells that will form the notochord such that by the end of gastrulation, *TBXT* expression is restricted to the notochord progenitors and in a small population of cells known as the neuromesodermal progenitors (NMPs) in the tailbud, which will form the tail somites and neural tube. TBXT maintains this tailbud progenitor cell population, and mutations in *TBXT* therefore abolish tail outgrowth [8]. As the progenitor pool is depleted and tailbud growth terminates, *TBXT* expression ceases in the tailbud, but remains in the notochord. As development proceeds, the notochord regresses except for some cells that remain in the nucleus pulposus of the intervertebral disc (IVD), which maintain *TBXT* expression into adulthood [9].

More recently, *TBXT* has been implicated in cancer biology due to its aberrant expression in various tumors, where it acts as both an oncogene and a tumor suppressor depending on the cancer type. TBXT is a critical oncogene in chordoma, a rare bone cancer that is thought to develop from the notochordal remnants present in adult IVDs [10]. *TBXT* is highly expressed in chordoma, and it serves as a diagnostic marker distinguishing them from other similar tumors like chondrosarcomas [3]. TBXT is also essential for chordoma cell survival and proliferation. Targeted degradation of TBXT protein arrests proliferation and induces senescence, and causes cell death when combined with inhibitors of anti-apoptotic proteins [11]. Recent advances in drug discovery have accordingly focused on targeting *TBXT* in chordoma [4], and this may also open routes to therapy in other cancers, since TBXT contributes to epithelial-to-mesenchymal transition (EMT) and metastasis in many

epithelial cancers. For instance, breast tumors overexpress TBXT, where high expression correlates with poor prognosis, and TBXT promotes proliferation and migration by regulating downstream targets such as *E2F3*, a transcription factor involved in cell cycle progression [12]. In non-small cell lung cancer (NSCLC), *TBXT* expression correlates with lymph node metastasis and appears to promote metastasis through upregulating mesenchymal and repressing epithelial gene expression [13, 14]. In prostate cancer, nuclear *TBXT* is correlated with tumor invasion and cytoplasmic *TBXT* with highly aggressive tumors [15].

In contrast, *TBXT* functions as a tumor suppressor in gliomas [16]. It is downregulated in glioma cells relative to normal brain tissues, and its loss correlates with increased tumor aggressiveness and poor patient prognosis. Re-expression of *TBXT* in glioma cells reduces tumorigenesis by inducing autophagy, which suggests a protective role in this context [16]. *TBXT* expression is largely absent in normal adult tissues, which makes it an attractive therapeutic target, and small molecule and protein inhibitors offer promising avenues where *TBXT* acts as an oncogene [17–20], although its context-dependent role calls for a nuanced approach. Transcription factors of this class have nonetheless proved hard to inhibit directly. A tumor that depends on TBXT is, however, equally dependent on mechanisms that establish and maintain its expression, and those mechanisms therefore represent a second class of therapeutic target. Few studies, however, have asked how *TBXT* expression is initially upregulated and then maintained in expressing cancers, or how it is silenced in glioma. We argue that identifying these mechanisms is a therapeutic question as much as a mechanistic one, since it would provide additional avenues for targeting *TBXT* that do not depend on inhibiting the protein itself.

3. Regulation of *TBXT* expression

3.1. Regulation by signaling pathways during vertebrate embryonic development

Animal models, and more recently human models of early development such as gastruloids, have been instrumental in uncovering how *TBXT* expression is regulated during embryogenesis. As discussed below, these models have shown that *TBXT* is initially induced in response to signals that drive mesendoderm formation and patterning, including Activin/Nodal, BMP, WNT and FGF, while later, during tail bud outgrowth, *TBXT* is also regulated by retinoic acid (RA). Throughout this review we describe regulation as direct where a pathway effector binds an identified cis-regulatory element at the *TBXT* locus, where mutation or deletion of that element abolishes the response, or where TBXT is induced within a time frame consistent with an immediate-early response, ideally in the presence of a protein synthesis inhibitor. We describe it as indirect or undetermined where a reported change in *TBXT* transcript or protein level following pathway manipulation does not separate direct transcriptional regulation from downstream cascade effects.

NODALs and ACTIVIN are secreted ligands of the transforming growth factor β (TGF-β) family that signal through type I and type II TGF-β receptors and downstream effectors, SMAD2 and SMAD3 (mothers against decapentaplegic homologs 2 and 3) [21]. TBXT is a direct transcriptional target of ACTIVIN/NODAL signaling in early embryos (e.g., [22, 23]). In *Xenopus*, Activin and several Nodal-related ligands are sufficient to induce *tbxt* expression in explant assays, while inhibiting Activin/Nodal signaling results in reduced or absent *tbxt* expression during blastula and gastrula stages (e.g., [24–26]). Similarly, in zebrafish Nodal-related 1 and 2 act redundantly to regulate *tbxta* expression in the dorsal mesoderm [27]. In mouse embryos, *Tbxt* is also a target of NODAL signaling, with mutations that disrupt NODAL signaling resulting in reduced or absent *Tbxt* expression

and impaired mesoderm formation during gastrulation or in mouse embryonic stem cells (ESCs) differentiated towards mesoderm (e.g., [28]). Likewise, in human stem cell-derived gastruloid models, inhibition of NODAL signaling leads to downregulation of *TBXT* expression [29].

Bone morphogenetic proteins (BMPs) are also members of the TGF-β superfamily, which act through the downstream effectors, SMAD1, SMAD5 and SMAD9. BMP signaling plays a key role in mesodermal patterning and as such contributes to regulating *TBXT* expression. Studies in *Xenopus* and zebrafish indicate Bmp signaling induces expression (e.g., [30]), whereas inhibition of Bmp activity directly downregulates *tbxta* expression in zebrafish [31]. However, in NMPs of the zebrafish tailbud, BMP is thought to act indirectly to regulate *tbxta* expression through upregulation of Wnt signaling [30]. In early mouse embryos and mammalian stem cell differentiation models, BMP signaling similarly regulates *TBXT* expression indirectly, through upregulation of WNT and NODAL signaling [32, 33]. On the other hand, in cultures of mouse tailbud-derived mesoderm progenitors, BMP acts directly, since BMP signaling can induce *Tbxt* expression in the presence of protein synthesis inhibitors [34].

Fibroblast growth factors (FGFs), also secreted ligands, signal through receptor tyrosine kinases leading to activation of several downstream pathways, including the mitogen-activated protein kinase (MAPK) pathway, the phosphoinositide 3-kinase (PI3K)/protein kinase B (AKT) pathway, and the phospholipase Cγ (PLCγ) pathway [35]. FGF signaling plays multiple roles in vertebrate embryogenesis, notably in mesoderm formation, cell migration through the primitive streak and tail elongation [36, 37]—all processes in which *TBXT* is critically involved. During mesoderm formation, FGF signaling induces and is required for *tbxt* expression in both zebrafish and *Xenopus* embryos. Genetic or pharmacological inhibition of FGF signaling leads to reduced *tbxt* expression while ectopic Fgf expression in zebrafish embryos or in *Xenopus* explants is sufficient to induce *tbxt* [38, 39]. In mouse, FGF is also essential for *Tbxt* expression regulation. *Fgfr1* mutant embryos lack *Tbxt* expression in the primitive streak (excluding the node), and conditional removal of *Fgf8* and *Fgf4* during early gastrulation results in the absence of tailbud *Tbxt* expression by the end of gastrulation, while notochord expression persists [40]. The effect of FGF signaling on mesoderm formation appears to act primarily through the MAPK/extracellular signal-regulated kinase (ERK) kinase (MEK) pathway since inhibition of MAPK or MEK reduces *Tbxt* expression in *Xenopus* embryos and mouse gastruloids, whereas inhibition of PI3K/AKT does not [41, 42]. A positive feedback loop between Tbxt and Fgf is also important for maintenance of *tbxt* expression during gastrulation in *Xenopus* [43, 44]. However, in zebrafish this relationship shifts during tailbud outgrowth such that Fgf negatively regulates *tbxta* expression, with loss of Fgf signaling after the 8-somite stage causing upregulation of *tbxta* in the tailbud [45].

WNTs, which are also secreted ligands, signal by binding to Frizzled (FZD) receptors and low-density lipoprotein receptor-related protein 5/6 (LRP5/6) co-receptors [46], leading to stabilization of β-catenin (CTNNB1). Stabilized CTNNB1 translocates to the nucleus and complexes with T-cell factor/lymphoid enhancer-binding factor (TCF/LEF) transcription factors at target gene regulatory regions, including *TBXT*, to activate transcription. During mouse embryogenesis, WNT signaling is required to maintain, but not initiate, *Tbxt* expression in the primitive streak. In *Wnt3a* mutant embryos, *Tbxt* expression is progressively lost from the primitive streak starting at somitogenesis, while axial mesoderm (notochord) expression remains intact [47–49]. In *Xenopus* embryos, overactivation of Wnt signaling is sufficient to induce *tbxt*, whilst inhibition of Wnt signaling leads to downregulation of *tbxt* in the marginal zone during gastrulation [50]. By contrast, in zebrafish, *tbxta* expression in early embryos depends on intracellular Ctnnb1 activity, but is

not activated by extracellular Wnt signaling [51]. During tailbud outgrowth in zebrafish, on the other hand, Tbxt and Wnt act in a positive feedback loop to maintain each other's expression in NMPs [52, 53], highlighting the context-dependent action of WNT signaling.

Mechanotransduction also appears to regulate *TBXT* expression through CTNNB1. In both human gastruloid models and during gastrulation in zebrafish, mechanical tension at the cell membrane releases CTNNB1 from adherens junctions allowing it to enter the nucleus, resulting in upregulation of *TBXT* expression [51, 54, 55].

RA signaling, which is critical for posterior development in vertebrate embryos, acts to repress *TBXT* expression, although it is not known if this regulation is direct [7]. In zebrafish embryos, RA treatment during somitogenesis results in the loss of *tbxta* expression in the tailbud, although not in the notochord [53]. Similarly, RA treatment of mammalian gastruloids reduces *Tbxt* expression in a dose- and time-dependent manner [56, 57].

3.2. Regulation at cis-regulatory elements during vertebrate embryonic development

These different signals that regulate *TBXT* expression must then be transduced to the DNA via transcription factor binding at CREs [58]. Studies show that distinct CREs, including promoters, enhancers and silencers, are responsible for expression of *TBXT* in different regions of the embryo and respond to the different signals discussed above, and that organisms employ both conserved and non-conserved CREs for this expression.

In mouse, a CRE (*T-streak*) spanning approximately 540 bp upstream and 115 bp downstream of the *Tbxt* transcription start site (TSS) drives expression of a reporter in the primitive streak from the beginning of gastrulation in the same pattern as the endogenous *Tbxt* gene ([47–49]; **Figure 1**; **Table 1**). Reporter gene expression persists in the non-axial mesoderm during gastrulation but is absent in the node and notochord precursors. Following gastrulation, expression continues in the tailbud but not the notochord, indicating that the regulatory elements necessary for notochord expression are not present in this proximal promoter region [47–49]. *T-streak* contains TCF/LEF binding sites responsive to WNT signaling (**Figure 1**; **Table 1**). When these sites are mutated in reporter constructs, reporter expression is initiated but then lost in the mesoderm from late gastrulation, indicating that WNT signaling is essential for maintaining *Tbxt* expression through the TCF/LEF sites [48, 49, 59]. Experiments with mouse embryonic stem cells differentiated to mesoderm indicate NODAL and WNT signaling cooperate to regulate *Tbxt* expression. CTNNB1 binding recruits or stabilizes SMAD2/3 at the *Tbxt* promoter region, and SMAD2/3 then recruits the histone H3 lysine 27 trimethylation (H3K27me3) demethylase KDM6B (JMJD3) to remove repressive marks and activate *Tbxt* transcription [60] (**Figure 1**).

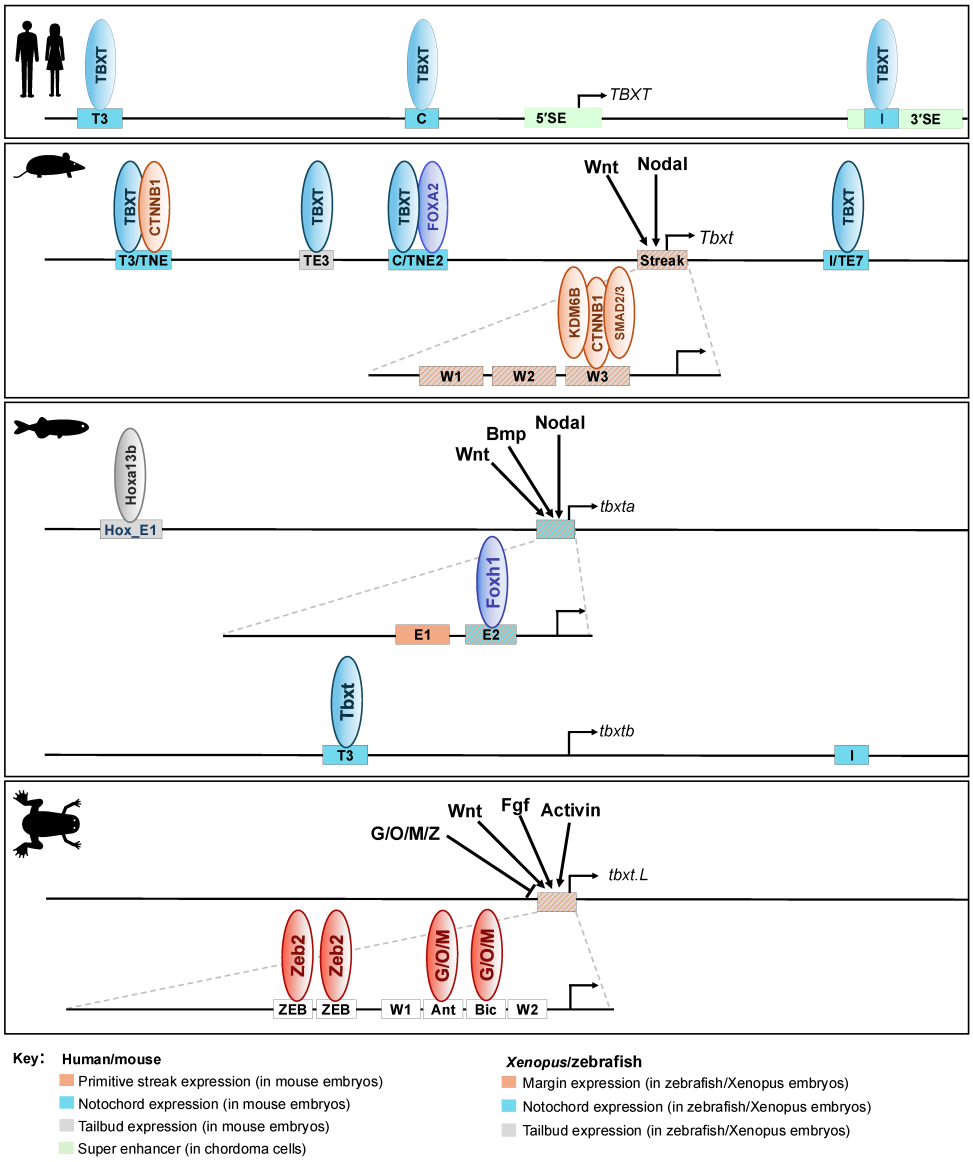


Figure 1. Schematic of the *TBXT* locus in human (*TBXT*), mouse (*Tbxt*), zebrafish (*tbxta* and *tbxtb*) and *Xenopus laevis* (*tbxt.L*). Boxes show identified cis-regulatory elements (CREs); their coordinates and supporting evidence are listed in **Table 1**. CREs are colored by the expression domain they drive: orange, primitive streak (mouse) or embryonic margin (zebrafish and *Xenopus*); cyan, notochord; gray, tailbud; green, super-enhancers in chordoma cells (5′SE and 3′SE). Hatched orange-gray box indicates primitive streak or margin plus tailbud, hatched orange-cyan box indicates primitive streak or margin plus notochord. White boxes indicate sites with no demonstrated expression domain. T3, C and I are conserved notochord enhancers. In mouse, TNE (within T3), TNE2 (containing C) and TE7 (within I) are notochord enhancers, and TE3 is a tailbud neuromesodermal progenitor enhancer. Mouse W1–W3 are TCF/LEF binding sites, and *Xenopus* W1 and W2 are Wnt-responsive sites. Zebrafish E1 and E2 are Bmp/Wnt-responsive and Nodal-responsive, respectively, and Hox_E1 is a tailbud enhancer bound by Hoxa13b. *Xenopus* ZEB, Ant and Bic denote ZEB-family and Antennapedia- and Bicoid-type homeodomain-binding sites, respectively. Ovals show transcription factors and chromatin regulators that bind the CREs: blue, TBXT; orange, CTNNB1, SMAD2/3 and KDM6B; purple, FOXA2 (mouse) and Foxh1 (zebrafish); gray, Hoxa13b; red, repressors. G/O/M/Z denotes Gsc, Otx2, Mix1 and Zeb2, and G/O/M denotes Gsc, Otx2 and Mix1. Straight arrows show positive signaling inputs, bar-headed lines show repression and bent arrows mark transcription start sites. Gray dashed lines link promoter regions to their expanded views. Positions are schematic and not to scale. SEs: super-enhancers. Species silhouettes were created using Claude (Opus 5).

Table 1. Identified CREs, their genomic positions, activity and factors that bind them in human, mouse, zebrafish and *Xenopus*. Coordinates are given relative to the following genome assemblies: human GRCh38, mouse GRCm38, zebrafish GRCz11, and *Xenopus laevis* XENLA_10.1 (Xenopus_laevis_v10.1; GCF_017654675.1); obtained from Xenbase [61]. Note that the coordinates for elements originally described in earlier assemblies were converted using the UCSC LiftOver tool [62, 63] and checked by alignment of the published sequence to these assemblies.

Species (genome version)	CRE	Chr	Start	End	Drives expression in/responds to	Required for	Histone/TF binding	Evidence for element function	Comments	References
Human (GRCh38)	T3	chr6	166,244,611	166,245,019	Drives expression in notochord in zebrafish, axolotl and mouse embryos.	T-box binding sites required for notochord expression in zebrafish.	TBXT binding in chordoma cells (U-CH1) and hESCs differentiated to mesoderm.	Reporter assay with site mutation (zebrafish); TBXT binding (ChIP). Endogenous requirement not tested.	-	[64, 65]
Human (GRCh38)	C	chr6	166,193,623	166,195,166	Drives expression in notochord in zebrafish, axolotl and mouse embryos.	T-box binding sites required for notochord expression in zebrafish.	TBXT binding in chordoma cells (U-CH1) and hESCs differentiated to mesoderm.	Reporter assay with T-box site mutation (zebrafish); TBXT binding (ChIP). Endogenous requirement not tested.	-	[64, 65]
Human (GRCh38)	5′SE	chr6	166,162,765	166,174,510	Element not tested.	Not tested for this element.	Extended H3K27ac in chordoma cells (multiple cell lines and patient samples); TBXT binding in hESCs differentiated to mesoderm.	Chromatin signature (extended H3K27ac) in chordoma and TBXT binding (ChIP) in mesodermal cells only. Element not tested in a reporter. Endogenous requirement not tested.	Spans TSS in chordoma cells.	[11, 17, 64]
Human (GRCh38)	I	chr6	166,121,608	166,122,211	Drives expression in notochord in zebrafish, axolotl and mouse embryos.	T-box binding sites required for notochord expression in zebrafish.	TBXT binding in chordoma cells (U-CH1) and hESCs differentiated to mesoderm.	Reporter assay with T-box site mutation (zebrafish); TBXT binding (ChIP). Endogenous requirement not tested.	Located in chordoma downstream super enhancer (3′SE).	[64, 65]

Table 1. *Cont.*

Species (genome version)	CRE	Chr	Start	End	Drives expression in/responds to	Required for	Histone/TF binding	Evidence for element function	Comments	References
Human (GRCh38)	3′SE	chr6	166,109,512	166,126,946	Element not tested.	*TBXT* expression in chordoma cell line.	Extended H3K27ac binding in chordoma cells (multiple cell lines and patient samples); TBXT binding in chordoma cells (U-CH1) and hESCs differentiated to mesoderm.	CRISPRi (dCas9–KRAB) at the endogenous locus; chromatin signature (extended H3K27ac); TBXT binding (ChIP). Element not tested in a reporter.	Located 60 kb downstream of *TBXT* gene in chordoma cells.	[11, 17]
Mouse (GRCm38)	T3	chr17	8,395,859	8,397,354	Drives expression in notochord in mouse embryos.	Required in combination with C and I for notochord expression of *Tbxt* and posterior tail formation.	TBXT binding in in vitro differentiated notochord cells and NMPs.	Endogenous deletion (required in combination with C and I); reporter assay; TBXT binding (ChIP).	Element incorporates TNE.	[64, 66]
Mouse (GRCm38)	TNE	chr17	8,396,196	8,397,101	Drives expression in notochord in mouse embryos.	Normal tail formation and notochord progenitor specification. Required in combination with TNE2 for trunk/tail notochord formation.	TBXT binding in in vitro differentiated notochord cells and NMPs. CTNNB1 binding in in vitro differentiated NMPs.	Endogenous deletion; reporter assay; *TBXT* and CTNNB1 binding (ChIP).	Element is within T3.	[66, 67]
Mouse (GRCm38)	TE3	chr17	8,408,925	8,409,565	Drives expression in tailbud in mouse embryos.	Deletion of TE3 does not result in a phenotype.	TBXT binding in in vitro differentiated NMPs. H3K4me1 in in vitro differentiated notochord cells.	Endogenous deletion (no phenotype); reporter assay; TBXT binding and H3K4me1 (ChIP).	-	[66]
Mouse (GRCm38)	TNE2	chr17	8,415,515	8,420,121	Drives expression in notochord in mouse embryos.	Normal tail formation and notochord cell differentiation. Required in combination with TNE for trunk/tail notochord formation.	TBXT binding in mESCs differentiated to mesoderm; *TBXT* and FOXA2 in vitro differentiated notochord cells. H3K4me1, H3K27ac in in vitro differentiated notochord cells.	Endogenous deletion; reporter assay; *TBXT* and FOXA2 binding, H3K4me1 and H3K27ac (ChIP).	Element incorporates C.	[66, 68]

Table 1. *Cont.*

Species (genome version)	CRE	Chr	Start	End	Drives expression in/responds to	Required for	Histone/TF binding	Evidence for element function	Comments	References
Mouse (GRCm38)	C	chr17	8,416,977	8,417,336	Does not drive expression in mouse or zebrafish embryos.	Required in combination with T3 and I for notochord expression of *Tbxt* and posterior tail formation.	TBXT binding in mESCs differentiated to mesoderm; *TBXT* in in vitro differentiated notochord cells.	Endogenous deletion (required in combination with T3 and I); reporter assay negative; TBXT binding (ChIP).	Element is within TNE2.	[64, 68]
Mouse (GRCm38)	T_Streak	chr17	8,433,880	8,434,538	Drives expression in primitive streak and tailbud in mouse embryos. Responds to Wnt (*CTNNB1* overexpression).	Not tested.	TBXT binding in mESCs differentiated to mesoderm; *TBXT* in in vitro differentiated notochord cells.	Reporter assay; TBXT binding (ChIP). Endogenous requirement not tested.	-	[47, 59, 66, 68]
Mouse (GRCm38)	W1	chr17	8,434,021	8,434,027	Element not tested individually.	Required in combination with W3 for tailbud expression in the context of reporter construct similar to T-streak.	Recombinant LEF and CTNNB1 bind to region containing W1, W2 and W3 (EMSA). Recombinant LEF binds to W1 (EMSA).	Site mutation within a reporter (in combination with W3); binding by EMSA only.	W1 is element described as distal TCF/LEF site in [49].	[49]
Mouse (GRCm38)	W2	chr17	8,434,108	8,434,115	Element not tested individually for expression. Responds to Wnt (*CTNNB1* overexpression).	Not tested.	Recombinant LEF and CTNNB1 bind to region containing W1, W2 and W3 (EMSA).	Reporter responsiveness only; binding by EMSA only. Requirement not tested.	W2 is element described as TCF-site II in [59].	[59]
Mouse (GRCm38)	W3	chr17	8,434,188	8,434,195	Element not tested individually for expression. Responds to Wnt (*CTNNB1* overexpression).	Expression in the tailbud in the context of reporter construct similar to T-streak. Not required for initiation of expression in the primitive streak.	Recombinant LEF and CTNNB1 bind to region containing W1, W2 and W3 (EMSA). CTNNB1, SMAD2/3 and JMJD3 bind region upstream of *Tbxt* TSS which contains W3 in mouse ESCs differentiated to mesoderm.	Site mutation within a reporter; binding by EMSA, and by ChIP in surrounding region (CTNNB1, SMAD2/3, JMJD3).	W3 is element described as proximal TCF/LEF site in Yamaguchi et al. [49], described as −117/−110 in Galceran et al. and described as TCF-site I in [59].	[48, 49, 59, 60]

Table 1. *Cont.*

Species (genome version)	CRE	Chr	Start	End	Drives expression in/responds to	Required for	Histone/TF binding	Evidence for element function	Comments	References
Mouse (GRCm38)	I	chr17	8,447,788	8,448,149	Drives expression in notochord in mouse embryos.	Required in combination with T3 and C for notochord expression of *Tbxt* and posterior tail formation.	TBXT binding in mESCs differentiated to mesoderm. TBXT binding in in vitro differentiated notochord cells.	Endogenous deletion (required in combination with T3 and C); reporter assay; TBXT binding (ChIP).	Element incorporates TE7.	[64, 66]
Mouse (GRCm38)	TE7	chr17	8,447,847	8,448,139	Drives expression in notochord in mouse embryos.	Deletion of TE7 does not result in a phenotype.	TBXT binding in in vitro differentiated notochord cells (ChIP-seq).	Endogenous deletion (no phenotype); reporter assay; TBXT binding (ChIP).	Element is within I.	[66]
Zebrafish (GRCz11)	tbxtb_T3	chr13	4,425,688	4,426,329	Drives expression in notochord in zebrafish embryos.	Not tested.	Tbxta binding in zebrafish gastrula embryos.	Reporter assay; Tbxta binding (ChIP). Endogenous requirement not tested.	-	[64, 69]
Zebrafish (GRCz11)	tbxtb_I	chr13	4,458,073	4,458,357	Drives expression in notochord in zebrafish embryos.	Not tested.	No binding of Tbxta (at 8 hpf).	Reporter assay only. Endogenous requirement not tested.	-	[64, 69]
Zebrafish (GRCz11)	tbxta_1 kb	chr19	14,191,523	14,192,565	Drives expression in margin (stronger in dorsal–lateral margin) during gastrulation and in notochord after gastrulation in zebrafish embryos. Responds to Nodal signaling.	Not tested.	See E2 element below.	Reporter assay, including pathway responsiveness. Endogenous requirement not tested.	Contains E2 but not E1 enhancer.	[31]

Table 1. *Cont.*

Species (genome version)	CRE	Chr	Start	End	Drives expression in/responds to	Required for	Histone/TF binding	Evidence for element function	Comments	References
Zebrafish (GRCz11)	tbxta_2.1 kb	chr19	14,191,517	14,193,640	Drives expression in margin at gastrula stages and notochord after gastrulation in zebrafish embryos. Responds to Nodal, Wnt and BMP signaling.	Not tested.	See E2 element below.	Reporter assay, including pathway responsiveness. Endogenous requirement not tested.	Contains both E1 and E2 enhancer.	[31]
Zebrafish (GRCz11)	tbxta_hox_E1	chr19	14,215,593	14,216,674	Drives expression in tailbud (NMPs) during somitogenesis in zebrafish embryos.	Robust *tbxta* expression in the tailbud and formation of mesoderm in posterior of embryo.	H3K4me1, H3K27ac and Hoxa13b occupancy in isolated zebrafish tailbuds at the 15–18-somite stage.	Endogenous deletion; reporter assay; Hoxa13b binding, H3K4me1 and H3K27ac (CUT&RUN).	-	[70]
Zebrafish (GRCz11)	tbxta_E1	chr19	14,192,576	14,192,614	Element not tested individually for expression. Responds to BMP and Wnt signaling.	Not tested.	-	Reporter responsiveness only, within a larger fragment. Element not tested individually; no binding data.	-	[31]
Zebrafish (GRCz11)	tbxta_E2	chr19	14,192,257	14,192,306	Element not tested individually. Responds to Nodal signaling. Fox motif required for Nodal responsiveness.	Notochord expression after gastrulation (in context of 2.1 kb reporter).	Foxh1 binding in zebrafish blastula/gastrula embryos.	Site mutation within a reporter (Fox motif); Foxh1 binding (ChIP).	-	[23, 31]
Xenopus laevis (XENLA_10.1)	2.1 kb	chr5L	57,449,502	57,451,718	Drives expression in ventral–lateral margin during gastrulation and in tailbud in *X. laevis* embryos. Responds to FGF and Activin signaling. Repressed by Gsc, Otx2, Mix1.	Not tested.	See Ant/Bic/SIP sites below.	Reporter assay, including pathway responsiveness and repression. Endogenous requirement not tested.	-	[39, 71]

Table 1. *Cont.*

Species (genome version)	CRE	Chr	Start	End	Drives expression in/responds to	Required for	Histone/TF binding	Evidence for element function	Comments	References
Xenopus laevis (XENLA_10.1)	946 bp	chr5L	57,449,393	57,450,338	Element not tested individually for expression. Responds to Wnt and Activin signaling. TCF sites required for Wnt responsiveness.	Not tested.	See Ant/Bic/SIP sites below.	Reporter responsiveness with site mutation (TCF sites), within a larger fragment. Endogenous requirement not tested.	Element referred to as 802 bp in original publication.	[50]
Xenopus laevis (XENLA_10.1)	430 bp	chr5L	57,449,506	57,449,935	Drives expression in ventral–lateral margin during gastrulation in *X. laevis* embryos (tailbud expression not assayed). Responds to FGF and Activin signaling. Repressed by Gsc. Ant and Bic sites required for repression.	Not tested.	See Ant/Bic/SIP sites below.	Reporter assay with site mutation (Ant and Bic). Endogenous requirement not tested.	Element referred to as −381 bp in original publications.	[39, 71]
Xenopus laevis (XENLA_10.1)	Ant	chr5L	57,449,721	57,449,727	Element not tested individually.	Repression in dorsal mesoderm and ectoderm at mid-gastrulation (in context of 430 bp reporter construct).	Gsc, Otx2 and Mix1 (EMSA with construct containing both Ant and Bic site).	Site mutation within a reporter; binding by EMSA only (construct containing both Ant and Bic).	-	[39, 71]
Xenopus laevis (XENLA_10.1)	Bic	chr5L	57,449,708	57,449,714	Element not tested individually.	Repression enhancement in ventral mesoderm and ectoderm (in context of 430 bp reporter construct).	Gsc, Otx2 and Mix1 (EMSA with construct containing both Ant and Bic site).	Site mutation within a reporter; binding by EMSA only (construct containing both Ant and Bic).	-	[39, 71]

Table 1. *Cont.*

Species (genome version)	CRE	Chr	Start	End	Drives expression in/responds to	Required for	Histone/TF binding	Evidence for element function	Comments	References
Xenopus laevis (XENLA_10.1)	ZEB (CAGGTG)	chr5L	57,449,857	57,449,862	Element not tested individually.	Repression in ectoderm and endoderm at early gastrula stages (in context of 2.1 kb reporter construct).	ZEB2 (SIP1), in conjunction with other ZEB (CACCT) site (EMSA).	Site mutation within a reporter; binding by EMSA only (in conjunction with the ZEB (CACCT) site).	-	[71, 72]
Xenopus laevis (XENLA_10.1)	ZEB (CACCT)	chr5L	57,449,886	57,449,890	Element not tested individually.	Repression in ectoderm and endoderm at early gastrula stages (in context of 2.1 kb reporter construct).	ZEB2 (SIP1; EMSA).	Site mutation within a reporter; binding by EMSA only.	-	[71, 72]
Xenopus laevis (XENLA_10.1)	W1	chr5L	57,449,773	57,449,779	Element not tested individually for expression. Responds to Wnt signaling (Wnt8 and TCF3 overexpression).	Full activity of 946 bp reporter when both W1 and W2 mutated (luciferase assay).	Not tested.	Site mutation within a reporter (luciferase). Binding not tested; endogenous requirement not tested.	-	[50]
Xenopus laevis (XENLA_10.1)	W2	chr5L	57,449,649	57,449,655	Element not tested individually. Responds to Wnt signaling (Wnt8 and TCF3 overexpression).	Full activity of 946 bp reporter when both W1 and W2 mutated (luciferase assay).	Not tested.	Site mutation within a reporter (luciferase). Binding not tested; endogenous requirement not tested.	-	[50]

CRE: cis-regulatory element; Chr: chromosome; TSS: transcription start site; SE: super-enhancer; TF: transcription factor; ChIP: chromatin immunoprecipitation; EMSA: electrophoretic mobility shift assay; CUT&RUN: cleavage under targets and release using nuclease; CRISPRi: clustered regularly interspaced short palindromic repeats interference; dCas9: nuclease-deficient Cas9; KRAB: Krüppel-associated box; hESC/mESC: human/mouse embryonic stem cell; NMP: neuromesodermal progenitor; hpf: hours post-fertilization; BMP: bone morphogenetic protein; FGF: fibroblast growth factor; TCF/LEF: T-cell factor/lymphoid enhancer-binding factor; H3K4me1: histone H3 lysine 4 monomethylation; H3K27ac: histone H3 lysine 27 acetylation; UCSC: University of California Santa Cruz; –: not applicable.

More recently, studies have identified several CREs that regulate *Tbxt* expression in the notochord of mice (**Figure 1**). One such element, located approximately 13.5 kb downstream of the *Tbxt* TSS (designated *I* [64] which incorporates *TE7* [66]; **Table 1**; **Figure 1**) drives expression throughout the full length of the notochord. Another CRE, located approximately 37.8 kb upstream of the *Tbxt* TSS (designated *TNE* [66, 67] which lies within *T3* [64]) drives reporter gene expression in the notochord of the tail. An additional CRE approximately 17.4 kb upstream of the *Tbxt* TSS, designated *C* [64] lies within a larger region called *TNE2* [66], and while mouse *TNE2* can drive reporter expression in the tail notochord of mice, the shorter *C* region cannot, suggesting essential regulatory sequences for notochord expression lie outside of *C*. These elements nonetheless appear to work together to regulate expression. When *TNE* is deleted in mouse embryos using genome editing, *Tbxt* expression is reduced in the tail notochord [67]. However, when this deletion is combined with removal of *TNE2* or *C* and *I*, *Tbxt* expression is completely lost in both trunk and tail notochord cells ([64, 66]; **Table 1**).

Sequence analysis shows T3, C and I are conserved in humans [64], and human T3, C and I CREs drive reporter expression in the notochord of mouse, zebrafish and axolotl embryos, which might indicate they have similar activity during human embryogenesis, whereas the mouse C fragment lacks autonomous reporter activity in mouse and zebrafish embryos [64]. However, these studies did not examine gastrulation stages, so it is not known whether these CREs drive expression in the primitive streak/axial mesoderm during gastrulation. Much more also remains to be understood about the transcription factors and signals that regulate these CREs, although *TBXT* and CTNNB1 bind TNE in mouse stem cells differentiated to NMPs, consistent with a role for WNT signaling regulating *Tbxt* expression in the tailbud. *TBXT* also binds to enhancers T3, C and I in mouse embryonic stem cells differentiated to notochord precursors indicating it may regulate its own expression in these cells [66], as discussed further below.

In *Xenopus laevis*, a region approximately 400 bp upstream of the *X. laevis tbxt.L* TSS (*X. laevis* is allotetraploid and has two *tbxt* homeologs, *tbxt.L* and *tbxt.S*) drives reporter expression in the ventral–lateral marginal zone at gastrula stages and in the tailbud at later stages, but does not show dorsal marginal zone or notochord expression, indicating these control regions are elsewhere, as seen in mouse ([39, 71]; **Table 1**; **Figure 1**). As described above, Activin, Fgf and Wnt signaling activate *tbxt* expression in *Xenopus*, and the region approximately 400 bp to 250 bp upstream of the TSS responds to both Fgf and low levels of Activin signaling, similar to the endogenous gene, while Tcf/Lef binding sites at 120 bp and 245 bp upstream appear to mediate *tbxt.L* expression in response to Wnt signaling during gastrulation ([50]; **Table 1**).

In zebrafish, separate enhancers drive expression in the margin, notochord and tailbud (**Figure 1**). Marginal and notochord expression is mediated by the region between ~1.4 kb and 0.7 kb upstream of the *tbxta* TSS which contains a Nodal-responsive element (E2) and a Bmp/Wnt-responsive element (E1; [31]). The Nodal-responsive element is required for dorsal marginal and notochord expression of a reporter, but not ventral marginal expression, which is consistent with the fact that *tbxta* expression remains in the ventral margin in Nodal signaling mutant embryos [31]. In addition, conserved T3 and I enhancers located at approximately 14.5 kb upstream and 17.5 kb downstream of the TSS of zebrafish *tbxtb*—a *tbxt* ohnologue that has a similar expression pattern to and partially redundant function with *tbxta* [52]—have been shown to drive expression of a reporter in the notochord, similar to mouse embryos ([64]; **Figure 1**; **Table 1**). A tailbud enhancer in zebrafish is also located distally, at approximately 25 kb upstream of the *tbxta* TSS that is bound by Hoxa13b [70]. When this tailbud enhancer is deleted, *tbxta* expression in the tailbud is downregulated, resulting in abnormal somite formation and a shorter tail [70]. A distal enhancer at approximately 25.2 kb upstream of mouse *Tbxt* TSS (known as TE3 [66]; **Table 1**) also drives *Tbxt* expression in the mouse tailbud, although deletion of this CRE does not result in abnormal tailbud formation, indicating other regions are required for *Tbxt* expression leading to tailbud formation in mouse.

One feature of *TBXT* is that it autoregulates its own expression, both in development and in chordoma cancer (discussed further below). In a *Xenopus* explant assay, zebrafish *tbxta* expression induces *Xenopus tbxt* expression [44]. Conversely, inhibition of Tbxt activity downregulates *tbxt* in the dorsal/axial mesoderm, although

expression in the ventral–lateral mesoderm is normal, indicating either *Tbxt* does not autoregulate itself in ventral–lateral mesoderm or other regulatory mechanisms compensate for loss of *tbxt*, such as the expression of *tbxtb* in zebrafish [52]. In mouse *Tbxt* mutants, early *Tbxt* expression is normal but begins to decrease by the end of gastrulation and is absent from the notochord during somitogenesis [68], suggesting *TBXT* is required for maintaining its own expression in the notochord. Although not directly demonstrating autoregulation, TBXT binds multiple sites within its own locus in *Xenopus* and zebrafish embryos, as well as in mouse and human embryonic cells differentiated toward mesodermal lineages ([65–69, 73]; **Table 1**; **Figure 1**), suggesting there may be direct autoregulation during embryogenesis. In mouse this appears to be through TBXT recruiting p300 histone acetyltransferase to the *Tbxt* promoter region and creating a permissive chromatin environment for expression [68].

Repression also plays a crucial role. In zebrafish, a 2.1 kb sequence upstream of the *tbxta* TSS drives reporter expression in the embryonic margin during gastrulation. When only 1 kb of upstream sequence is used, ectopic expression appears in the endoderm, suggesting that repressive elements preventing endodermal expression lie between 2.1 kb and 1 kb upstream of the TSS, although these are yet to be characterized [31]. Similarly, in *Xenopus*, a 2.1 kb upstream region of *tbxt.L* drives ectopic reporter expression in the animal and vegetal regions during the blastula stage, which resolves to the marginal zone by the onset of gastrulation, indicating repression of *tbxt* expression is both spatially and temporally regulated [71]. Further analysis of this region reveals several repressor binding sites, including Zeb (aka Sip) zinc finger binding sites and homeodomain binding sites, located approximately 400 bp upstream of the TSS (**Figure 1**). These elements likely ensure *tbxt.L* expression is restricted to the mesoderm at the beginning of gastrulation [71]. Additionally, homeodomain binding sites between approximately 150 bp and 250 bp upstream of the TSS appear to mediate repression of *tbxt* at high Activin levels, through recruitment of transcription factors such as Mix1, Otx2, and Gsc ([39, 71]; **Table 1**; **Figure 1**).

DNA methylation at CpG islands is a key mechanism for regulating gene expression, with promoter hypermethylation typically linked to transcriptional repression. During early development, the genome undergoes widespread demethylation after which de novo DNA methyltransferases such as DNMT3B establish lineage-specific methylation patterns. This includes methylation at the *TBXT* locus. However, during mesoderm differentiation in human embryonic stem cells, a long non-coding RNA transcribed from the *TBXT* locus, lncRNA divergent activator of *TBXT* (*LNCDAT*; previously known as *yylncT*) interacts with DNMT3B and prevents local methylation of the *TBXT* locus, resulting in *TBXT* expression [74].

3.3. Regulation by signaling pathways in cancer

While multiple signaling pathways directly regulate *TBXT* expression during development, their involvement in directly controlling *TBXT* expression during cancer is much less clear. Studies have linked developmental signaling pathways to *TBXT* regulation in cancer, but with one exception none assays *TBXT* within a time frame that would indicate direct regulation, and no study has yet shown binding of a transcription factor in response to signaling at a CRE in the *TBXT* locus in a cancer cell. We summarize what is known below and in **Figure 2**, and give details, timings and evidence for direct regulation in **Table 2**.

Table 2. Signaling pathways characterized in different cancer cell models, including derived xenografts and the effect of inhibiting or activating these pathways on *TBXT* expression. For each model, the molecular readout (*TBXT* mRNA and/or protein) and the assay timing or model endpoint are given, together with an assessment of whether the study provides evidence for direct transcriptional regulation of *TBXT*, as defined in Section 3.1.

Signaling pathway	Cancer cell type	Cell line	Inhibition of signaling: method	Inhibition: outcome	Activation of signaling: method	Activation: outcome	Readout assayed	Time of TBXT assay after treatment	Evidence for direct regulation of *TBXT* transcription	Reference
FGF	Chordoma	JHC7, U-CH1, U-CH2	FGF2 neutralizing antibody, PD173074, PD0325901 or PD184352.	Downregulation of TBXT protein.	FGF2 ligand.	Upregulation of TBXT protein.	Protein.	48 h (inhibition); 24 h (FGF2).	Indirect or undetermined.	[75]
	Lung	NCI-H460	PD173074 or PD184352.	Downregulation of TBXT protein.	Na.	Na.	Protein.	48 h.	Indirect or undetermined.	[76]
		NCI-H460	FGFR1 siRNA.	Downregulation of TBXT mRNA and protein.	FGF1 ligand.	Upregulation of TBXT protein.	mRNA and protein (FGFR1 silencing); protein (FGF1 activation).	24 h (silencing, mRNA); 48 h (silencing, protein); 24 h FGF1 exposure (protein).	Indirect or undetermined.	[76]
		NCI-H460	FGFR1 shRNA.	Downregulation of TBXT protein (in xenograft tumor).	Na.	Na.	Protein.	Xenograft endpoint.	Indirect or undetermined.	[77]
		NCI-H226	FGFR1 siRNA, PD173074, or PD184352.	Downregulation of TBXT protein.	Na.	Na.	Protein.	48 h.	Indirect or undetermined. Protein-level readout only.	[76]
		NCI-H358	Na.	Na.	FGFR1 overexpression (stable).	Upregulation of *TBXT* mRNA.	mRNA.	Stable FGFR1 expression; mRNA assayed 24 h after shRNA step.	Indirect or undetermined.	[76]
		NCI-H441	Na.	Na.	FGFR1 overexpression (stable).	Upregulation of TBXT mRNA and protein.	mRNA and protein.	Stable FGFR1 expression.	Indirect or undetermined.	[76, 77]
PI3K/AKT	Chordoma	U-CH2	LY294002 or BEZ235.	Downregulation of TBXT mRNA; TBXT protein also reduced by BEZ235	Na.	Na.	mRNA and protein.	24 h (mRNA); protein timing Nr.	Indirect or undetermined.	[78]

Table 2. *Cont.*

Signaling pathway	Cancer cell type	Cell line	Inhibition of signaling: method	Inhibition: outcome	Activation of signaling: method	Activation: outcome	Readout assayed	Time of TBXT assay after treatment	Evidence for direct regulation of *TBXT* transcription	Reference
TGF-β	Prostate	DU145	SD-208.	Downregulation of TBXT mRNA.	TGF-β1 ligand.	Upregulation of *TBXT* mRNA and protein.	mRNA (inhibition); mRNA and protein (activation).	72 h.	Indirect or undetermined.	[79]
	Colorectal	SW480, SW620	SD-208.	Downregulation of TBXT mRNA (and protein for SW620).	Na.	Na.	mRNA and protein.	72 h.	Indirect or undetermined.	[79]
	Lung	NCI-H460	SD-208.	Downregulation of TBXT protein.	Na.	Na.	Protein.	72 h.	Indirect or undetermined.	[79]
WNT/CTNNB1	Chordoma	MUG-Chor1	XAV939 or IWP-2.	Upregulation of *TBXT* mRNA and protein (active CTNNB1 reduced).	Lithium chloride, BIO, CHIR99021 or LY2090314 (GSK3B inhibitors).	Downregulation of *TBXT* mRNA and protein (active CTNNB1 increased).	mRNA and protein.	24 h.	Indirect or undetermined. See Section 3.3 for further discussion.	[80]
		MUG-Chor1	Overexpression of *GSK3B*.	Downregulation of *TBXT* mRNA; slight (1.2-fold) upregulation of TBXT protein (active CTNNB1 slightly increased).	*GSK3B* siRNA.	Upregulation of TBXT mRNA and protein (no significant change in active CTNNB1).	mRNA and protein.	72 h (overexpression); 48 h (siRNA).	Indirect or undetermined. See Section 3.3 for further discussion.	[80]
		UM-Chor1	Na.	Na.	AR-A014418 (GSK3 inhibitor).	Downregulation of *TBXT* mRNA and protein (nuclear CTNNB1 decreased).	mRNA and protein.	24 h.	Indirect or undetermined. See Section 3.3 for further discussion.	[81]
	Colorectal	SW480	*CTNNB1* siRNA.	Downregulation of TBXT protein.	Na.	Na.	Protein	24 h.	Indirect or undetermined.	[82]
Retinoic acid	Glioma	U-373, SNB-19	Na.	Na.	Trans-retinoic acid.	Upregulation of TBXT mRNA.	mRNA.	24 h (sustained to 60 h).	Indirect or undetermined.	[83]

Table 2. *Cont.*

Signaling pathway	Cancer cell type	Cell line	Inhibition of signaling: method	Inhibition: outcome	Activation of signaling: method	Activation: outcome	Readout assayed	Time of TBXT assay after treatment	Evidence for direct regulation of *TBXT* transcription	Reference
EGFR	Chordoma	U-CH1, MUG-Chor1	Afatinib.	Downregulation of TBXT protein (U-CH1); no effect on TBXT mRNA (U-CH1 and MUG-Chor1).	Na.	Na.	mRNA and protein.	24 and 48 h (mRNA); protein time course includes 2, 8, 24 and 48 h.	Post-transcriptional: TBXT protein reduced, *TBXT* mRNA unchanged.	[84]
	Lung	A549	Tyrphostin (AG 1478).	Upregulation of TBXT mRNA.	Na.	Na.	mRNA.	2 weeks.	Indirect.	[85]
Hypoxia	Breast	MCF-7, T-47D	Na.	Na.	Hypoxia.	Upregulation of TBXT mRNA and protein.	mRNA and protein.	6 h.	Time frame is compatible with direct transcriptional upregulation, but no binding of HIF-1α or another effector at a TBXT CRE has been shown.	[86]

Na: not assessed in the study; Nr: not reported; FGF: fibroblast growth factor; FGFR: FGF receptor; MEK: MAPK/ERK kinase; ERK: extracellular signal-regulated kinase; MAPK: mitogen-activated protein kinase; PI3K: phosphoinositide 3-kinase; AKT: protein kinase B; TGF-β: transforming growth factor β; EGFR: epidermal growth factor receptor; CTNNB1: β-catenin; GSK3B: glycogen synthase kinase 3β; HIF-1α: hypoxia-inducible factor 1α; siRNA: small interfering RNA; shRNA: short hairpin RNA; CRE: cis-regulatory element; BIO: 6-bromoindirubin-3′-oxime.

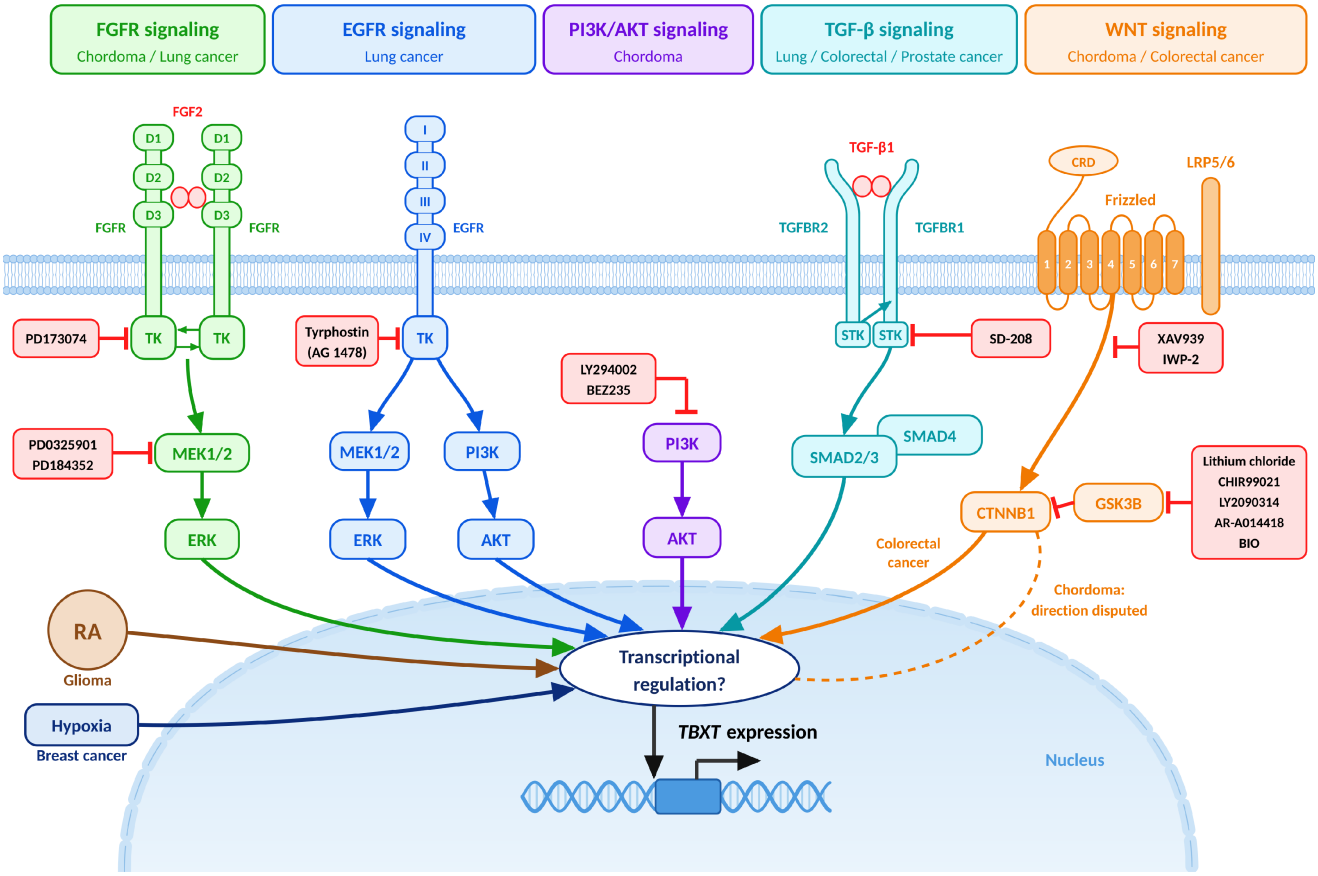


Figure 2. Signaling pathways and pharmacological modulators associated with *TBXT* expression in cancer. Supporting evidence is given in **Table 2**. Pathways are colored as follows: green, FGF/FGFR; blue, EGFR; purple, PI3K/AKT; teal, TGF-β/SMAD; orange, WNT; brown, retinoic acid (RA); navy, hypoxia. The membrane separates extracellular and intracellular components, and the pale blue compartment is the nucleus. The FGF2 and TGF-β1 ligands and the pharmacological modulators used in the cited studies are outlined in red. D1–D3 and I–IV denote FGFR and EGFR extracellular domains, respectively, and 1–7 denote Frizzled transmembrane helices. Solid arrows and inhibition bars show pathway activation and inhibition, respectively, and the dashed orange line indicates the unresolved WNT response in chordoma. The bent black arrow from the blue box on DNA marks *TBXT* expression. The inhibition bar from XAV939 and IWP-2 indicates inhibition of WNT signaling. IWP-2 inhibits PORCN and blocks WNT ligand secretion; XAV939 inhibits tankyrase (TNKS), promoting CTNNB1 degradation. The PI3K/AKT arm begins at PI3K because no upstream receptor or ligand has been established, and intermediaries linking RA and hypoxia to *TBXT* have not yet been characterized in cancer. The question mark in "Transcriptional regulation?" indicates that these responses have not been shown to involve direct effector binding at a *TBXT* cis-regulatory element. Cancer labels identify the models studied, not universal responses. FGF/FGFR: fibroblast growth factor/receptor; EGFR: epidermal growth factor receptor; MEK: MAPK/ERK kinase; MAPK: mitogen-activated protein kinase; ERK: extracellular signal-regulated kinase; PI3K: phosphoinositide 3-kinase; AKT: protein kinase B; TGF-β: transforming growth factor β; TGFBR1/2: TGF-β receptors 1/2; SMAD: mothers against decapentaplegic homolog; CRD: cysteine-rich domain; LRP5/6: low-density lipoprotein receptor-related proteins 5/6; TK: tyrosine kinase; STK: serine/threonine kinase; GSK3B: glycogen synthase kinase 3β; CTNNB1: β-catenin; PORCN: porcupine O-acyltransferase; BIO: 6-bromoindirubin-3′-oxime. The schematic was generated and iteratively revised using Claude (Opus 5).

Several studies have identified FGF signaling as a regulator of *TBXT* in cancer [2]. Chordoma cell lines secrete FGF2 and express multiple components of the pathway, including FGFR2, FGFR3, MEK and ERK [75], and most patient samples express at least one FGF receptor [87]. Accordingly, inhibition of FGF signaling in chordoma cell

lines reduces MEK and ERK phosphorylation and *TBXT* expression, and reduces cell proliferation while increasing apoptosis ([75]; **Table 2**). As in development, a positive feedback loop between FGF signaling and *TBXT* may operate in chordoma since knockdown of *TBXT* reduces FGF2 secretion and MEK/ERK phosphorylation [75].

FGF signaling also regulates *TBXT* expression in lung cancer. Activating the pathway, with FGF1 or by overexpressing FGFR, induces *TBXT* expression in lung cancer cell lines with low endogenous *TBXT*, such as H358 and H441, and lines with higher endogenous *TBXT*, including H226 and H460, are more sensitive to the FGFR and MAPK inhibitors ([76, 77]; **Table 2**).

The PI3K/AKT signaling pathway has also been implicated in upregulating *TBXT* in chordoma ([78]; **Table 2**). Inhibiting PI3K/AKT signaling in U-CH2 chordoma cells reduces *TBXT* expression and suppresses cell proliferation [78]. Interestingly, in the breast cancer cell lines MCF-7 and T-47D, elevated *TBXT* levels are associated with increased AKT phosphorylation [86], which suggests a possible positive feedback loop between TBXT and AKT signaling.

TGF-β treatment induces *TBXT* expression across a range of prostate and lung cancer cell lines (**Table 2**). Interestingly, induction follows a bell-shaped dose–response curve, with peak expression at intermediate levels of TGF-β1 ([79]; **Table 2**), a pattern that resembles the dose-dependent regulation of *TBXT* by ACTIVIN and NODAL during development. Inhibiting TGF-β signaling downregulates *TBXT* mRNA or protein expression in prostate, colorectal and lung cancer cells [79]. Silencing *TBXT* reduces TGF-β1 promoter activity in reporter assays, indicating a possible positive feedback loop [79], and in U-CH2 chordoma cells silencing *TGF-β1* downregulates *TBXT* expression [10].

In contrast to the pathways above, the relationship between WNT signaling and *TBXT* regulation in chordoma is unresolved. In the canonical WNT pathway, GSK3B acts within a destruction complex that phosphorylates CTNNB1 and targets it for degradation. WNT ligand binding inhibits this complex, so that CTNNB1 accumulates, enters the nucleus and activates transcription. Pharmacological inhibition of *GSK3B* is therefore widely used as a WNT agonist and would be expected to stabilize CTNNB1 and activate the pathway. Two studies report that pharmacological inhibition of *GSK3B* lowers *TBXT* expression. In UM-Chor1 and MUG-Chor1 cells, such inhibition lowered *TBXT* mRNA and protein, while in MUG-Chor1 cells the WNT inhibitors XAV939 and IWP-2 raised both ([80, 81]; **Table 2**). However, the two studies read this result differently because they report opposite CTNNB1 responses. In UM-Chor1 cells, pharmacological inhibition of *GSK3B* reduced nuclear CTNNB1, read as WNT inhibition lowering *TBXT* [81], while increased active CTNNB1 in MUG-Chor1 after treatment was read as WNT activation lowering *TBXT* [80].

Cell viability is a further consideration. GSK3B inhibitors reduced viability in both studies, whereas XAV939 and IWP-2 increased it [80, 81]. *TBXT* levels therefore track the viability of the cultures in these experiments, and an effect on *TBXT* transcription cannot be separated from the consequences of reduced viability. Genetic manipulation is no easier to reconcile. Knockdown of *GSK3B* with siRNA increased *TBXT* mRNA and protein, yet left active CTNNB1 unchanged, suggesting the effect is not through canonical WNT signaling ([80]; **Table 2**). One possible explanation is that the small molecules used in these studies inhibit GSK3A as well as GSK3B, whereas the siRNA targets GSK3B alone. Overexpression of GSK3B reduced *TBXT* mRNA by approximately 90% while slightly increasing TBXT protein, and raised rather than lowered CTNNB1 ([80]; **Table 2**). The direction and mechanism of WNT regulation of *TBXT* in chordoma therefore remains undetermined. In SW480 colorectal cancer cells, by contrast, knockdown of *CTNNB1* reduced TBXT protein ([82]; **Table 2**), although *TBXT* mRNA was not assessed, so whether this acts at the level of transcriptional regulation is unknown.

RA signaling suppresses *TBXT* expression in animal models. In glioma cell lines, however, RA treatment induced *TBXT* expression at 24 h ([83]; **Table 2**), which may implicate RA in regulating *TBXT* expression in healthy brain tissue, where TBXT is typically expressed.

The epidermal growth factor (EGF) signaling pathway has also been investigated. In lung cancer, inhibition in the low *TBXT*-expressing A549 cell line increased *TBXT* expression and cell invasiveness, but only after two weeks of exposure, which suggests an indirect consequence of treatment ([85]; **Table 2**). Supporting this, in U-CH1 chordoma cells, EGFR inhibition left *TBXT* mRNA levels unchanged, while the accompanying loss of TBXT protein was prevented by proteasome or autophagy inhibitors, indicating a post-transcriptional effect ([84]; **Table 2**).

Hypoxia is a common feature of the tumor microenvironment. In breast cancer cell lines, six hours of hypoxia raised *TBXT* mRNA and protein, a timeframe that could indicate direct upregulation of *TBXT* transcription ([86]; **Table 2**). The increase in *TBXT* was accompanied by upregulation of mesenchymal markers and downregulation of epithelial markers, and silencing *TBXT* under hypoxic conditions reversed these changes.

Overall, the regulation of *TBXT* expression by signaling pathways is context-dependent and differs across cancer types. Most studies have assessed *TBXT* expression 24 h or more after pathway activation or inhibition, leaving it unclear whether these effects reflect direct regulation of *TBXT* transcription or downstream, indirect mechanisms (**Table 2**). The exception is the response to hypoxia in breast cancer cells, where *TBXT* is induced within six hours, which could indicate a direct effect [86]. However, the effector of this response is yet to be identified.

3.4. Regulation at cis-regulatory elements in cancer

If signaling is direct, downstream effectors of each pathway would transduce the signal to CREs at the *TBXT* locus. However, there has been little research into CREs controlling *TBXT* expression in cancer and whether these are conserved with development. The best studied is chordoma, where several chordoma cell lines and patient samples carry super-enhancers (SEs) within a 1.5 Mb active regulatory region surrounding *TBXT* [11, 17].

Extended histone H3 lysine 27 acetylation (H3K27ac) marks, indicating an SE, lie both upstream of the *TBXT* TSS (5′SE) and approximately 60 kb downstream of the *TBXT* gene (3′SE; **Figure 1** and **Figure 3**; **Table 1**). Transcription-associated cyclin-dependent kinases (tCDKs) regulate gene transcription and are associated with SEs, and CDK7, CDK9, CDK12 and CDK13, alongside TBXT itself, are selective dependencies in chordoma cells [17]. Inhibiting tCDKs with THZ1 downregulates *TBXT* and induces apoptosis, but affects only endogenous *TBXT* and not *TBXT* expressed from an exogenous promoter, and ectopic *TBXT* partially rescues the resulting loss of viability, indicating that the antiproliferative effect depends in part on loss of SE-driven *TBXT* transcription [17]. In a separate approach, targeting the 3′SE in CH22 chordoma cells with a nuclease-deficient CRISPR-associated protein 9 (dCas9) fused to the Krüppel-associated box (KRAB) repressor domain downregulates *TBXT* mRNA to a level comparable to repressing the *TBXT* promoter itself, indicating this region regulates *TBXT* expression in chordoma [11]. Our preliminary analysis of publicly available histone H3 lysine 27 acetylation (H3K27ac) chromatin immunoprecipitation sequencing (ChIP-seq) data across *TBXT*-expressing epithelial cancers, including breast, colorectal and lung cancer, does not show extended H3K27ac equivalent to the chordoma 3′SE, although *TBXT*-expressing NCI-H460 lung cancer cells have H3K27ac at enhancer I, the developmental notochord enhancer [64], and all the epithelial cancer cells show some H3K27ac decoration more distally (**Figure 3**). Consistent with this, mapping of chromatin contacts from the *TBXT* promoter in NCI-H460 cells found no extended contacts in the 3′SE equivalent region [88]. ChIP-seq datasets from mouse and zebrafish also show no evidence of a downstream SE at the *TBXT* locus during development (**Figure 3**) [66, 89]. These observations might suggest the extended 3′SE at the *TBXT* locus is specific to chordoma.

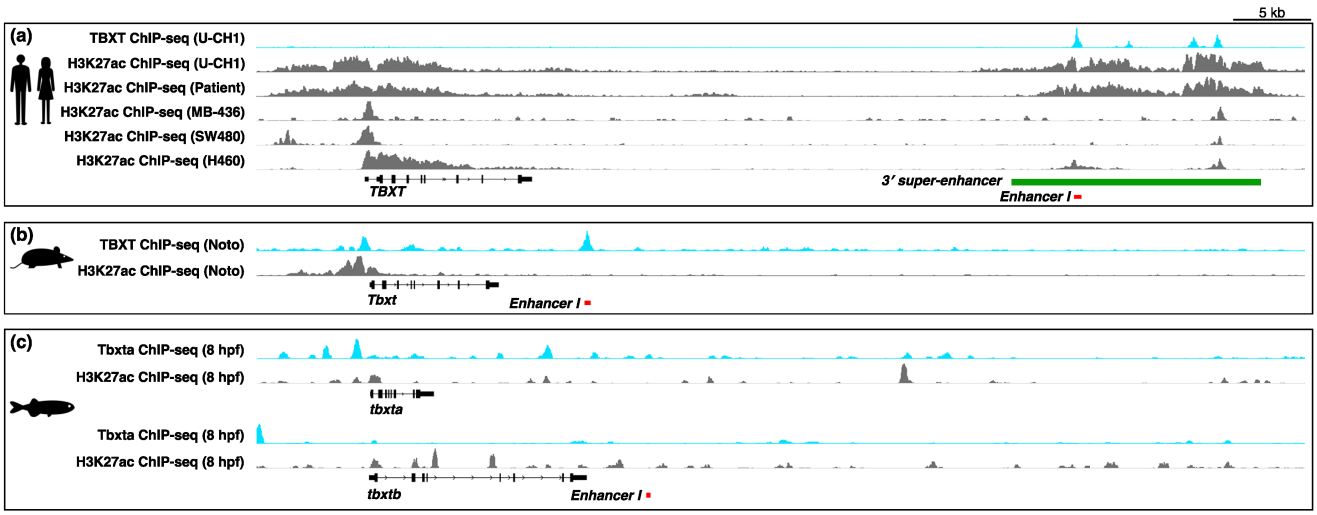


Figure 3. Representative chromatin immunoprecipitation sequencing (ChIP-seq) tracks at *TBXT* loci in (**a**) human, (**b**) mouse and (**c**) zebrafish. ChIP-seq files were downloaded from the Gene Expression Omnibus (GEO) or DANIO-CODE [89] and visualized in the Integrative Genomics Viewer (IGV) [90], based on data reported for chordoma [17] (GSE109971), breast cancer [91] (GSE85158), colorectal cancer [92, 93] (GSE179461; GSE73319), lung cancer [94] (GSE143653), mouse [66] (GSE235030) and zebrafish [69, 89] (DCD000136SR; DCD000407SR). Representative tracks show ChIP-seq signal for TBXT (human and mouse) or Tbxta (zebrafish) in cyan and for histone H3 lysine 27 acetylation (H3K27ac) in gray. Samples are abbreviated in the track labels as follows: U-CH1: U-CH1 chordoma cell line; Patient: patient chordoma sample; MB-436: MDA-MB-436 breast cancer cell line; SW480: colorectal cancer cell line; H460: NCI-H460 lung cancer cell line; Noto: mouse embryonic stem cells (ESCs) differentiated to notochord-like cells; 8 hpf: zebrafish embryos at 8 hours post-fertilization. The zebrafish panel shows the *tbxta* locus (upper tracks) and the *tbxtb* locus (lower tracks). In the gene models, boxes indicate exons, lines indicate introns and arrowheads indicate the direction of transcription. The green bar marks the chordoma 3′ super-enhancer, and red bars mark the conserved enhancer I, which lies downstream of *TBXT* in human, *Tbxt* in mouse and *tbxtb* in zebrafish. Scale bar, 5 kb. Species silhouettes were created using Claude (Opus 5).

TBXT regulates its own expression in the CH22 chordoma cell line, as it does during development [11]. TBXT binds at several locations across the 3′SE, including enhancer I ([17, 64, 95]; **Table 1**; **Figure 3**). Binding of TBXT at the 3′SE plays a role in expression autoregulation through formation of a transcriptional condensate containing *TBXT* and bromodomain-containing protein 4 (BRD4), a transcriptional co-activator, at the *TBXT* locus [11].

Epigenetic repression of *TBXT* is also used as a mechanism to regulate *TBXT* expression. The non *TBXT*-expressing osteosarcoma line U2OS carries high levels of the repressive marks H3K27me3 and H3K9me2 at the *TBXT* promoter, whereas the *TBXT*-expressing chordoma lines U-CH1, MUG-Chor1 and UM-Chor1 carry much lower levels [96]. When the combined activity of histone H3K27 demethylases, KDM6A and KDM6B is inhibited in U-CH1 cells with KDOBA67, an inhibitor of KDM6A/B, H3K27me3 levels at the *TBXT* promoter increase while active marks, H3K27ac and H3K4me3, decrease, leading to a decrease in *TBXT* mRNA levels and induction of apoptosis [96]. Both KDM6A and KDM6B bind to the *TBXT* promoter region and *3′SE* in U-CH1 cells, and inhibition of KDM6A/B reduces *TBXT* pre-mRNA, a measure of nascent transcription, within 3 h of treatment, indicating that reduction in histone methylation by KDM6A/B has a direct effect on *TBXT* transcription, although the effector of this is unknown [96]. Interestingly, it has also been observed that in chordoma patient samples, low levels of H3K27me3 are associated with poor prognosis [97]. Taken together these results indicate that removal of repressive marks decorating the *TBXT* promoter is required for its expression in chordoma cells.

DNA methylation at the *TBXT* locus may also play a role in regulation of *TBXT* expression in chordoma. Differential methylation analysis at the *TBXT* promoter indicates it is hypomethylated in chordoma samples compared to

normal nucleus pulposus samples, and this hypomethylation is linked to the upregulation of *TBXT* [98]. Reduced methylation is also seen, however, in non *TBXT*-expressing mesenchymal tumors such as chondroblastomas, which may suggest regulation of *TBXT* expression by DNA methylation is context-dependent [96].

As observed in development, non-coding RNAs also regulate expression of *TBXT* in cancer. The long non-coding RNA, metastasis-associated lung adenocarcinoma transcript 1 (*MALAT1*), has been implicated in repressing *TBXT* expression in prostate cancer through the modulation of histone modifications. It interacts with enhancer of zeste homolog 2 (EZH2), a core component of the Polycomb repressive complex-2 (PRC2) that functions as a histone methyltransferase and promotes gene silencing [99]. Depletion of *MALAT1* through siRNA-mediated knockdown resulted in the derepression of EZH2 target genes, including *TBXT*. Chromatin immunoprecipitation assays corroborated these findings, demonstrating diminished recruitment of EZH2 to the *TBXT* promoter and reduced levels of H3K27me3 upon *MALAT1* knockdown in PC-3 and C4-2 prostate cancer cell lines. *MALAT1* has also been reported to exert oncogenic effects across other cancers, including lung and colorectal cancer [100], although whether it regulates *TBXT* expression in these cancers is yet to be determined.

Taken together, *TBXT* expression in chordoma depends on removal of repressive chromatin marks at its promoter and on an extended 3′SE with no identified counterpart in development or in other *TBXT*-expressing cancers. This suggests a therapeutic avenue, since the regulatory machinery sustaining *TBXT* expression may prove more tractable than the protein itself. Outside chordoma, the only candidate elements reported are regions that contact the *TBXT* promoter and carry active chromatin marks in NCI-H460, a *TBXT*-expressing lung cancer cell line, and these have not yet been tested functionally [88], while regulation by DNA methylation and by non-coding RNAs remains poorly characterized.

3.5. Comparing regulation of *TBXT* expression in development and cancer

The signaling pathways implicated in *TBXT* regulation are largely the same in both development and cancer (**Table 3**). NODAL/ACTIVIN and the wider TGF-β family, FGF, WNT, BMP and RA all have reported effects on *TBXT* expression in embryos, and TGF-β, FGF, WNT, EGF and RA have reported effects in cancer cells. However, the effects themselves vary with context. FGF and TGF-β family signaling promote *TBXT* expression in both embryos and cancer cells, whereas RA represses *TBXT* in the zebrafish embryonic tailbud and mammalian gastruloids and induces it in glioma cells. Context-dependence of this kind is also seen within conditions. In zebrafish, FGF promotes *tbxta* expression during gastrulation and represses it in the tailbud after the 8-somite stage, and in cancer, manipulation of WNT signaling has been reported to have opposite effects on *TBXT* expression in chordoma and colorectal cells. The output of a given pathway at the *TBXT* locus therefore appears to depend on the cell type in which it acts.

Table 3. Comparison of pathways and mechanisms regulating *TBXT* expression during vertebrate development and in cancer. For each input, the reported effect on *TBXT* expression, evidence for direct regulation and an assessment of whether the mechanism is conserved is given for both contexts. Evidence of direct regulation is assessed as defined in Section 3.1.

Input	Effect on TBXT in development	Evidence for direct regulation of TBXT in development	Effect on TBXT in cancer	Evidence for direct regulation of TBXT in cancer	Conserved between development and cancer?
NODAL/ACTIVIN (TGF-β family)	Induces *TBXT*; required for *TBXT* expression in the early embryo in multiple species.	Direct. Site mutation within a reporter (zebrafish E2 Fox motif); effector binding (ChIP: Foxh1; SMAD2/3 with CTNNB1 at the mouse promoter region).	TGF-β1 induces *TBXT* in prostate and lung cell lines (bell-shaped dose response); SD-208 or TGF-β1 silencing reduces *TBXT* in prostate, colorectal, lung and chordoma cells.	None. Expression change, assayed ≥ 24 h.	Direction conserved (activating); dose dependence mirrors development. Whether SMADs act at *TBXT* CREs in cancer is unknown.
BMP	Induces *tbxt*/*tbxta* in *Xenopus* and zebrafish gastrula; maintains tailbud progenitors in mouse.	Direct. Reporter responsiveness (zebrafish E1) and induction in the presence of a protein synthesis inhibitor (mouse tailbud). Indirect in NMPs and mammalian stem cell models, where BMP acts via WNT and NODAL.	Not examined.	Not examined.	Unknown; not tested in cancer.
FGF	Induces and maintains *TBXT* during mesoderm formation; positive feedback with TBXT. Represses *tbxta* in the zebrafish tailbud after the 8-somite stage.	Direct for upregulation. Induction in the presence of a protein synthesis inhibitor, and FGF-responsive CRE identified in *Xenopus*.	Promotes *TBXT* in chordoma (FGF2/FGFR/MEK/ERK) and in lung cancer (FGFR1); positive feedback with TBXT reported in chordoma.	None. Expression change, assayed ≥ 24 h; several studies report protein-level readouts only.	Direction conserved (activating), and feedback loop with TBXT is conserved, but whether mechanism is conserved is unknown.
WNT/CTNNB1	Required to maintain, but not to initiate, *Tbxt* in the mouse primitive streak; induces *tbxt.L* in *Xenopus*; positive feedback with *Tbxt* in the zebrafish tailbud.	Direct. Site mutation within a reporter (mouse and *Xenopus*); CTNNB1 binding at *TNE* (ChIP).	Promotes *TBXT* expression in SW480 colorectal cells. Reported in both directions in chordoma depending on WNT pathway manipulation.	None. Expression change, assayed ≥ 24 h.	Direction conserved (activating) in SW480 colorectal cancer cells and development. Direction unresolved in chordoma (see Section 3.3 for discussion).
Retinoic acid	Represses *TBXT* in the tailbud of zebrafish and mouse embryos, and in gastruloids.	Indirect or undetermined. No responsive element identified.	Induces *TBXT* in glioma lines U-373 and SNB-19.	None. Expression change, assayed ≥ 24 h.	Direction reversed in glioma vs. development.
EGF/EGFR	Not examined.	Not examined.	EGFR inhibition upregulates *TBXT* in A549 lung cells after 2 weeks; afatinib lowers TBXT protein but not mRNA in chordoma cells at 24 h.	None. Note that in chordoma regulation is post-transcriptional (TBXT protein decreased but mRNA unchanged at 24 h).	Unknown; not tested in development.

Table 3. *Cont.*

Input	Effect on TBXT in development	Evidence for direct regulation of TBXT in development	Effect on TBXT in cancer	Evidence for direct regulation of TBXT in cancer	Conserved between development and cancer?
Hypoxia	Not examined.	Not examined.	Upregulates *TBXT* mRNA and protein in MCF-7 and T-47D breast cancer cells (**Table 2**) and drives EMT.	Undetermined—response within 6 h is compatible with an immediate-early effect, but no effector binding at a *TBXT* CRE has been shown (see **Table 2**).	Unknown; not tested in development; possible direct transcriptional regulation in breast cancer.
Mechanotransduction	Releases CTNNB1 from adherens junctions, upregulates *TBXT* in zebrafish gastrulae and human gastruloids.	Inferred to be direct. Potential to act through CTNNB1 and TCF/LEF sites (see above), but has not been tested.	Not examined.	Not examined.	Unknown; not tested in cancer.
TBXT autoregulation	TBXT binds multiple sites across its own locus in *Xenopus*, zebrafish, mouse and human cells; required to maintain its own expression in late gastrulation; recruits p300 to the mouse *Tbxt* promoter.	Direct. TBXT binding at identified elements (ChIP: *T3, TNE*).	TBXT binds several sites across the chordoma 3′SE, including enhancer *I*, and forms a transcriptional condensate with BRD4 at the *TBXT* locus.	Direct. TBXT binding at the chordoma 3′SE (ChIP).	Conserved.
Chromatin and epigenetic regulation	KDM6B recruited to *Tbxt* promoter region 1 to remove H3K27me3; *LNCDAT* (*yylncT*) sequesters DNMT3B to keep the locus unmethylated.	Direct. Effector recruitment to the locus demonstrated in both cases (KDM6B; DNMT3B sequestration by *LNCDAT*).	KDM6A/B bind the *TBXT* promoter and 3′SE in U-CH1 chordoma cells; inhibition raises H3K27me3. *MALAT1* recruits EZH2 to the *TBXT* promoter in prostate cancer. *TBXT* promoter is hypomethylated in chordoma.	Direct. KDM6A/B and MALAT1–EZH2 binding at the *TBXT* locus, with H3K27me3 change on KDM6A/B inhibition.	Conserved.
Cis-regulatory elements	Distinct CREs drive primitive streak, notochord and tailbud expression; conserved (*T3, C, I*) and species-specific elements identified in mouse, human, zebrafish and *Xenopus* (see **Table 1** and **Figure 1**).	Direct. Reporter assays and endogenous deletions.	Chordoma 3′SE extended H3K27ac, TBXT binding, and functionally validated (CRISPRi). Candidate CREs mapped in NCI-H460 but remain functionally untested. No CREs identified in other *TBXT*-expressing cancers.	Direct for the chordoma 3′SE only (CRISPRi).	Partially conserved. Enhancer I (notochord enhancer) located within chordoma 3′SE, but there is no evidence of an extended 3′SE in development.

TGF-β: transforming growth factor β; BMP: bone morphogenetic protein; FGF: fibroblast growth factor; FGFR: FGF receptor; MEK: MAPK/ERK kinase; MAPK: mitogen-activated protein kinase; ERK: extracellular signal-regulated kinase; EGF/EGFR: epidermal growth factor/receptor; PI3K: phosphoinositide 3-kinase; AKT: protein kinase B; CTNNB1: β-catenin; TCF/LEF: T-cell factor/lymphoid enhancer-binding factor; ChIP: chromatin immunoprecipitation; CRISPRi: clustered regularly interspaced short palindromic repeats interference; CRE: cis-regulatory element; SE: super-enhancer; NMP: neuromesodermal progenitor; KDM6A/B: lysine demethylases 6A/6B; *LNCDAT*: lncRNA divergent activator of *TBXT*; DNMT3B: DNA methyltransferase 3B; EZH2: enhancer of zeste homolog 2; p300: E1A-binding protein p300 histone acetyltransferase; BRD4: bromodomain-containing protein 4; SMAD: mothers against decapentaplegic homolog; H3K27me3/ac: histone H3 lysine 27 trimethylation/acetylation.

How these pathways reach the *TBXT* locus has been studied much more extensively in embryos than in cancer cells. In embryos, the effectors of several pathways bind identified CREs, and the elements concerned have been mapped in four species (**Table 1**; **Figure 1**). In cancer, the chordoma 3′SE is the only element to have been functionally tested, and the developmental CREs listed in **Table 1** have not been functionally assayed in cancer cells. Enhancer I, a notochord enhancer, lies within the chordoma 3′SE and is bound by TBXT in chordoma cells ([11, 17]; **Figure 1** and **Figure 3**), although its activity in chordoma has not been assessed independently of the surrounding SE. Whether cancers that express *TBXT* use CREs that also operate in the embryo, or elements with no developmental role, therefore remains to be determined.

TBXT does, however, autoregulate its own expression both during development and in chordoma (Sections 3.2 and 3.4). In the embryo this appears to be restricted to the notochordal lineage (Section 3.2). The notochord does not switch off *TBXT* at the end of embryogenesis. Subpopulations of adult human nucleus pulposus cells retain notochordal marker expression, including *TBXT*, although *TBXT* can acquire local H3K27me3 enrichment and be downregulated as discs age and degenerate [9, 101]. Chordoma is thought to arise from notochordal remnants but whether the extended 3′SE at the *TBXT* locus is present in notochordal cells of the adult disc has not been examined. Whether autoregulation operates in these cells has also not been tested, so it is not known whether the loop itself differs between them and chordoma cells.

The chromatin state of a locus is not independent of the physical and metabolic condition of the cell in which it sits. Two such influences are worth noting, although neither has been examined at the *TBXT* locus in embryos or in cancer. The first is the biophysical environment of the tumor. As discussed above (Section 3.1), mechanical tension promotes nuclear accumulation of *CTNNB1* and upregulation of *TBXT* during gastrulation [51, 54, 55], and tumors are characteristically stiffer than the tissues from which they arise, a consequence in part of collagen crosslinking [102]. Such cues could act on the epigenetic mechanisms described above, since mechanical state regulates PRC2 activity and H3K27me3 levels during lineage commitment [103], and AKT phosphorylates EZH2 to lower H3K27me3 at PRC2 target genes [104]. Given that the *TBXT* promoter carries H3K27me3 in non-expressing cells and that TBXT is a PRC2/EZH2 target in prostate cancer [96, 99], this offers a possible route by which extracellular cues might relieve Polycomb-mediated repression at *TBXT*.

The second is metabolic state. As discussed, KDM6A and KDM6B bind the *TBXT* promoter and 3′SE, and their combined activity is required for *TBXT* expression in chordoma [96]. KDM6A in particular has been shown to act as a direct oxygen sensor independently of hypoxia-inducible factor (HIF) [105], so low oxygen might be predicted to raise H3K27me3 at the *TBXT* promoter and lower *TBXT* expression. However, in breast cancer cells, hypoxia raises *TBXT* expression within six hours [86], implying that activating inputs outweigh any loss of demethylase activity in that context. Separately, assembly of the chordoma SEs, which are defined by extended H3K27ac, may depend on the availability of glucose-derived nuclear acetyl coenzyme A (acetyl-CoA) [106], while histone methylation more broadly is sensitive to methionine and S-adenosylmethionine (SAM) availability [107]. To our knowledge no study has manipulated oxygen tension or metabolite availability and then measured demethylase or PRC2 occupancy, H3K27me3 or H3K27ac at the *TBXT* locus, in either embryogenesis or cancer.

4. Conclusions

The route from an extracellular signal to *TBXT* transcription has not been fully mapped in either development or cancer. Ligands of the ACTIVIN/NODAL, BMP, FGF, WNT and RA pathways activate cascades that converge on effector transcription factors, which bind CREs at the *TBXT* locus and recruit co-activators and chromatin-modifying complexes. In development this chain has been established for some elements, including the Nodal-responsive E2 element of zebrafish *tbxta* and the TCF/LEF sites of the mouse T-streak element. However, in cancer none of these steps has been connected. No effector has been identified for any pathway, the CRE

through which it would act has not been mapped, and the timescale of most experiments cannot separate direct transcriptional regulation from the downstream consequences of manipulating a pathway.

The cis-regulatory evidence in cancer is confined to chordoma. The 3′SE has been functionally validated by dCas9-KRAB-mediated repression and by its role in *TBXT* autoregulation and BRD4 recruitment, but our preliminary analysis of publicly available H3K27ac data suggests the lack of an equivalent region in other *TBXT*-expressing cancers, nor in mouse or zebrafish embryos (**Figure 3**). No CRE has been functionally validated in any other *TBXT*-expressing cancer, and none of the developmental enhancers in **Table 1** have been tested in a cancer cell. It therefore remains unknown whether *TBXT* expression in cancer reflects reactivation of developmental regulatory programs or the engagement of cancer-specific elements.

Resolving these questions would widen the potential routes by which *TBXT* might be targeted. Chordoma cells are dependent on continued *TBXT* expression, and lowering *TBXT* reduces cell viability, while in carcinoma cell lines, *TBXT* knockdown reduces proliferation, migration and invasion. Both tCDK inhibition and targeted degradation disrupt the loop through which TBXT maintains its own expression in chordoma and downstream transcriptional program, forming a basis for strategies directed at *TBXT* and its autoregulatory feedback loop. Identifying the cis-regulatory mechanisms that sustain *TBXT* expression across a range of cancer types and in patient-derived material, including the contributions of signaling pathways, effector transcription factors and epigenetic regulators, would extend the points and cell types in which this loop might be interrupted. Progress will depend on experiments that measure nascent *TBXT* transcription, test pathway responsiveness in the presence of protein synthesis inhibitors, and map effector binding across the *TBXT* locus in cancer cells. However, any such approach would need to take account of the context-dependence described above, such as TBXT acting as a tumor suppressor in glioma.

Acknowledgments

We gratefully acknowledge Yaguang Si and Daniel Freed at the Chordoma Foundation for their helpful comments on a draft of this manuscript. The authors acknowledge the use of the AI tools ChatGPT (GPT-6.1 Sol) for language editing, scientific proofreading, reference checks and preparation of the revised **Figure 1**, and Claude (Opus 5) for generating **Figure 2** and the species silhouettes depicted in **Figure 1** and **Figure 3**. These tools were applied to enhance clarity and scholarly tone and to aid in figure preparation, and the authors take responsibility for checking the scientific content and approving the final text and figures. The authors fully support Academia.edu Journals' adherence to COPE guidelines on AI in publication ethics and confirm that this use has been managed responsibly and ethically.

Funding

This research was sponsored by the Chulabhorn Royal Academy for A.K.

Author contributions

Conceptualization, F.C.W.; writing—original draft preparation, M.H. and A.K.; writing—review and editing, F.C.W. and A.K.; visualization, A.K.; supervision, F.C.W.; project administration, F.C.W.; funding acquisition, A.K. All authors have read and agreed to the published version of the manuscript.

Conflict of interest

The authors declare that they have no competing interests, and that the funding sponsors played no role in the study's conception, design, execution, or interpretation, or with the writing of this manuscript.

Data availability statement

No new data was created in this study. The publicly available datasets reanalyzed in **Figure 3** have been made available within publicly accessible repositories: ChIP-seq datasets in the NCBI Gene Expression Omnibus under accession numbers GSE109971, GSE85158, GSE179461, GSE73319, GSE143653 and GSE235030, available at https://www.ncbi.nlm.nih.gov/geo/; and zebrafish ChIP-seq datasets in the DANIO-CODE Data Coordination Center under accession numbers DCD000136SR and DCD000407SR, available at https://danio-code.zfin.org/.

Publisher's note

Academia.edu Journals stays neutral regarding jurisdictional claims in published maps and institutional affiliations. All claims expressed in this article are solely those of the authors and do not necessarily represent those of their affiliated organizations, or those of the publisher, the editors, and the reviewers. Any product that may be evaluated in this article, or claim that may be made by its manufacturer, is not guaranteed or endorsed by the publisher.

Copyright

© 2026 copyright by the authors. This article is an open access article distributed under the terms and conditions of the Creative Commons Attribution (CC BY) license.

References

1. Korzh V. Never-ending story of Brachyury: from short-tailed mice to tailless primates. Cells Dev. 2024; 178: 203896. doi: 10.1016/j.cdev.2023.203896
2. Chen M, Wu Y, Zhang H, Li S, Zhou J, Shen J. The roles of embryonic transcription factor BRACHYURY in tumorigenesis and progression. Front Oncol. 2020; 10: 961. doi: 10.3389/fonc.2020.00961
3. Ma T, Bai J, Zhang Y. Current understanding of brachyury in chordoma. Biochim Biophys Acta Rev Cancer. 2023; 1878 (6): 189010. doi: 10.1016/j.bbcan.2023.189010
4. Zeinali M, Seraj FQM, Rawson C, Azab M, Karsy M. Systematic review of novel target therapies and clinical trials in chordoma. Clin Neurol Neurosurg. 2025; 259: 109222. doi: 10.1016/j.clineuro.2025.109222
5. Tecimel D, Seven D, Türe U, Bayrak ÖF. The molecular landscape of chordoma: current frontiers from multi-omics to artificial intelligence. Biochim Biophys Acta Rev Cancer. 2026; 1881 (5): 189678. doi: 10.1016/j.bbcan.2026.189678
6. Bruce AEE, Winklbauer R. Brachyury in the gastrula of basal vertebrates. Mech Dev. 2020; 163: 103625. doi: 10.1016/j.mod.2020.103625
7. Martins-Costa C, Wilson V, Binagui-Casas A. Neuromesodermal specification during head-to-tail body axis formation. In: Mallo M, editor. Vertebrate pattern formation. London, UK: Academic Press; 2024. p. 232–71. doi: 10.1016/bs.ctdb.2024.02.012

8. Martin BL, Steventon B. A fishy tail: insights into the cell and molecular biology of neuromesodermal cells from zebrafish embryos. Dev Biol. 2022; 487: 67–73. doi: 10.1016/j.ydbio.2022.04.010
9. Richardson SM, Ludwinski FE, Gnanalingham KK, Atkinson RA, Freemont AJ, Hoyland JA. Notochordal and nucleus pulposus marker expression is maintained by sub-populations of adult human nucleus pulposus cells through aging and degeneration. Sci Rep. 2017; 7 (1): 1501. doi: 10.1038/s41598-017-01567-w
10. Halvorsen SC, Benita Y, Hopton M, Hoppe B, Gunnlaugsson HO, Korgaonkar P, et al. Transcriptional profiling supports the notochordal origin of chordoma and its dependence on a TGFB1-TBXT network. Am J Pathol. 2023; 193 (5): 532–47. doi: 10.1016/j.ajpath.2023.01.014
11. Sheppard HE, Dall'Agnese A, Park WD, Shamim MH, Dubrulle J, Johnson HL, et al. Targeted brachyury degradation disrupts a highly specific autoregulatory program controlling chordoma cell identity. Cell Rep Med. 2021; 2 (1): 100188. doi: 10.1016/j.xcrm.2020.100188
12. Chen M, Liu J, Liang X, Huang Y, Yang Z, Lu P, et al. Knockdown of brachyury suppresses breast cancer cell proliferation and migration via targeting E2F3. J Oncol. 2022; 2022: 7913067. doi: 10.1155/2022/7913067
13. Xu K, Liu B, Liu Y. Impact of Brachyury on epithelial-mesenchymal transitions and chemosensitivity in non-small cell lung cancer. Mol Med Rep. 2015; 12 (1): 995–1001. doi: 10.3892/mmr.2015.3348
14. Fernando RI, Litzinger M, Trono P, Hamilton DH, Schlom J, Palena C. The T-box transcription factor Brachyury promotes epithelial-mesenchymal transition in human tumor cells. J Clin Investig. 2010; 120 (2): 533–44. doi: 10.1172/JCI38379
15. Pinto F, Pértega-Gomes N, Pereira MS, Vizcaíno JR, Monteiro P, Henrique RM, et al. T-box transcription factor brachyury is associated with prostate cancer progression and aggressiveness. Clin Cancer Res. 2014; 20 (18): 4949–61. doi: 10.1158/1078-0432.CCR-14-0421
16. Pinto F, Costa ÂM, Santos GC, Matsushita MM, Costa S, Silva VA, et al. The T-box transcription factor brachyury behaves as a tumor suppressor in gliomas. J Pathol. 2020; 251 (1): 87–99. doi: 10.1002/path.5419
17. Sharifnia T, Wawer MJ, Chen T, Huang Q-Y, Weir BA, Sizemore A, et al. Small-molecule targeting of brachyury transcription factor addiction in chordoma. Nat Med. 2019; 25 (2): 292–300. doi: 10.1038/s41591-018-0312-3
18. Chase DH, Bebenek AM, Nie P, Jaime-Figueroa S, Butrin A, Castro DA, et al. Development of a small molecule downmodulator for the transcription factor brachyury. Angew Chem Int Ed. 2024; 63 (14): e202316496. doi: 10.1002/anie.202316496
19. Umbaugh CS, Groth M, Erkut C, Lee KS, Marinho J, Linder S, et al. Selective targeting of TBXT with DARPins identifies regulatory networks and therapeutic vulnerabilities in chordoma. Sci Adv. 2025; 11 (36): eadu2796. doi: 10.1126/sciadv.adu2796
20. Newman JA, Gavard AE, Imprachim N, Aitkenhead H, Sheppard HE, Te Poele R, et al. Structural insights into human brachyury DNA recognition and discovery of progressible binders for cancer therapy. Nat Commun. 2025; 16 (1): 1596. doi: 10.1038/s41467-025-56213-1
21. El Kholtei J, Codina-Tobias M, Schier AF. Nodal signaling: a paradigm for TGFβ signaling in embryonic development. Annu Rev Cell Dev Biol. 2025; 41 (1): 45–88. doi: 10.1146/annurev-cellbio-112122-030209
22. Aragón E, Wang Q, Zou Y, Morgani SM, Ruiz L, Kaczmarska Z, et al. Structural basis for distinct roles of SMAD2 and SMAD3 in FOXH1 pioneer-directed TGF-β signaling. Genes Dev. 2019; 33 (21–2): 1506–24. doi: 10.1101/gad.330837.119
23. Dubrulle J, Jordan BM, Akhmetova L, Farrell JA, Kim SH, Solnica-Krezel L, et al. Response to Nodal morphogen gradient is determined by the kinetics of target gene induction. eLife. 2015; 4: e05042. doi: 10.7554/eLife.05042

24. Green JB, New HV, Smith JC. Responses of embryonic Xenopus cells to activin and FGF are separated by multiple dose thresholds and correspond to distinct axes of the mesoderm. Cell. 1992; 71 (5): 731–9. doi: 10.1016/0092-8674(92)90550-v
25. Luxardi G, Marchal L, Thomé V, Kodjabachian L. Distinct Xenopus Nodal ligands sequentially induce mesendoderm and control gastrulation movements in parallel to the Wnt/PCP pathway. Development. 2010; 137 (3): 417–26. doi: 10.1242/dev.039735
26. Takahashi S, Yokota C, Takano K, Tanegashima K, Onuma Y, Goto JI, et al. Two novel nodal-related genes initiate early inductive events in Xenopus Nieuwkoop center. Development. 2000; 127 (24): 5319–29. doi: 10.1242/dev.127.24.5319
27. Feldman B, Gates MA, Egan ES, Dougan ST, Rennebeck G, Sirotkin HI, et al. Zebrafish organizer development and germ-layer formation require nodal-related signals. Nature. 1998; 395 (6698): 181–5. doi: 10.1038/26013
28. Senft AD, Costello I, King HW, Mould AW, Bikoff EK, Robertson EJ. Combinatorial Smad2/3 activities downstream of Nodal signaling maintain embryonic/extra-embryonic cell identities during lineage priming. Cell Rep. 2018; 24 (8): 1977–85.e7. doi: 10.1016/j.celrep.2018.07.077
29. Warmflash A, Sorre B, Etoc F, Siggia ED, Brivanlou AH. A method to recapitulate early embryonic spatial patterning in human embryonic stem cells. Nat Methods. 2014; 11 (8): 847–54. doi: 10.1038/nmeth.3016
30. Row RH, Kimelman D. Bmp inhibition is necessary for post-gastrulation patterning and morphogenesis of the zebrafish tailbud. Dev Biol. 2009; 329 (1): 55–63. doi: 10.1016/j.ydbio.2009.02.016
31. Harvey SA, Tümpel S, Dubrulle J, Schier AF, Smith JC. *No tail* integrates two modes of mesoderm induction. Development. 2010; 137 (7): 1127–35. doi: 10.1242/dev.046318
32. Martyn I, Kanno TY, Ruzo A, Siggia ED, Brivanlou AH. Self-organization of a human organizer by combined Wnt and Nodal signalling. Nature. 2018; 558 (7708): 132–5. doi: 10.1038/s41586-018-0150-y
33. Turner DA, Rué P, Mackenzie JP, Davies E, Martinez Arias A. Brachyury cooperates with Wnt/β-catenin signalling to elicit primitive-streak-like behaviour in differentiating mouse embryonic stem cells. BMC Biol. 2014; 12 (1): 63. doi: 10.1186/s12915-014-0063-7
34. Sharma R, Shafer MER, Bareke E, Tremblay M, Majewski J, Bouchard M. Bmp signaling maintains a mesoderm progenitor cell state in the mouse tailbud. Development. 2017; 144 (16): 2982–93. doi: 10.1242/dev.149955
35. Liu X, Jing M, Yang Y, Jin Q, Feng B, Zhang P, et al. FGF family in health and disease. Mol Biomed. 2026; 7 (1): 33. doi: 10.1186/s43556-026-00429-0
36. Martin BL. Mesoderm induction and patterning: insights from neuromesodermal progenitors. Semin Cell Dev Biol. 2022; 127: 37–45. doi: 10.1016/j.semcdb.2021.11.010
37. McFann SE, Shvartsman SY, Toettcher JE. Putting in the Erk: growth factor signaling and mesoderm morphogenesis. In: Soriano PM, editor. Cell signaling pathways in development. Cambridge, MA, USA: Academic Press; 2022. p. 263–310. doi: 10.1016/bs.ctdb.2022.02.007
38. Griffin K, Patient R, Holder N. Analysis of FGF function in normal and *no tail* zebrafish embryos reveals separate mechanisms for formation of the trunk and the tail. Development. 1995; 121 (9): 2983–94. doi: 10.1242/dev.121.9.2983
39. Latinkic BV, Umbhauer M, Neal KA, Lerchner W, Smith JC, Cunliffe V. The Xenopus Brachyury promoter is activated by FGF and low concentrations of activin and suppressed by high concentrations of activin and by paired-type homeodomain proteins. Genes Dev. 1997; 11 (23): 3265–76. doi: 10.1101/gad.11.23.3265
40. Boulet AM, Capecchi MR. Signaling by FGF4 and FGF8 is required for axial elongation of the mouse embryo. Dev Biol. 2012; 371 (2): 235–45. doi: 10.1016/j.ydbio.2012.08.017
41. Umbhauer M, Marshall CJ, Mason CS, Old RW, Smith JC. Mesoderm induction in Xenopus caused by activation of MAP kinase. Nature. 1995; 376 (6535): 58–62. doi: 10.1038/376058a0

42. Underhill EJ, Toettcher JE. Control of gastruloid patterning and morphogenesis by the Erk and Akt signaling pathways. Development. 2023; 150 (16): dev201663. doi: 10.1242/dev.201663
43. Casey ES, O'Reilly MA, Conlon FL, Smith JC. The T-box transcription factor Brachyury regulates expression of eFGF through binding to a non-palindromic response element. Development. 1998; 125 (19): 3887–94. doi: 10.1242/dev.125.19.3887
44. Schulte-Merker S, Smith JC. Mesoderm formation in response to Brachyury requires FGF signalling. Curr Biol. 1995; 5 (1): 62–7. doi: 10.1016/s0960-9822(95)00017-0
45. Goto H, Kimmey SC, Row RH, Matus DQ, Martin BL. FGF and canonical Wnt signaling cooperate to induce paraxial mesoderm from tailbud neuromesodermal progenitors through regulation of a two-step epithelial to mesenchymal transition. Development. 2017; 144 (8): 1412–24. doi: 10.1242/dev.143578
46. Liu J, Xiao Q, Xiao J, Niu C, Li Y, Zhang X, et al. Wnt/β-catenin signalling: function, biological mechanisms, and therapeutic opportunities. Signal Transduct Target Ther. 2022; 7 (1): 3. doi: 10.1038/s41392-021-00762-6
47. Clements D, Taylor HC, Herrmann BG, Stott D. Distinct regulatory control of the Brachyury gene in axial and non-axial mesoderm suggests separation of mesoderm lineages early in mouse gastrulation. Mech Dev. 1996; 56 (1–2): 139–49. doi: 10.1016/0925-4773(96)00520-5
48. Galceran J, Hsu SC, Grosschedl R. Rescue of a Wnt mutation by an activated form of LEF-1: regulation of maintenance but not initiation of Brachyury expression. Proc Natl Acad Sci USA. 2001; 98 (15): 8668–73. doi: 10.1073/pnas.151258098
49. Yamaguchi TP, Takada S, Yoshikawa Y, Wu N, McMahon AP. T (Brachyury) is a direct target of Wnt3a during paraxial mesoderm specification. Genes Dev. 1999; 13 (24): 3185–90. doi: 10.1101/gad.13.24.3185
50. Vonica A, Gumbiner BM. Zygotic Wnt activity is required for Brachyury expression in the early Xenopus laevis embryo. Dev Biol. 2002; 250 (1): 112–27. doi: 10.1006/dbio.2002.0786
51. Brunet T, Bouclet A, Ahmadi P, Mitrossilis D, Driquez B, Brunet AC, et al. Evolutionary conservation of early mesoderm specification by mechanotransduction in Bilateria. Nat Commun. 2013; 4 (1): 2821. doi: 10.1038/ncomms3821
52. Martin BL, Kimelman D. Regulation of canonical Wnt signaling by Brachyury is essential for posterior mesoderm formation. Dev Cell. 2008; 15 (1): 121–33. doi: 10.1016/j.devcel.2008.04.013
53. Martin BL, Kimelman D. Brachyury establishes the embryonic mesodermal progenitor niche. Genes Dev. 2010; 24 (24): 2778–83. doi: 10.1101/gad.1962910
54. Muncie JM, Ayad NME, Lakins JN, Xue X, Fu J, Weaver VM. Mechanical tension promotes formation of gastrulation-like nodes and patterns mesoderm specification in human embryonic stem cells. Dev Cell. 2020; 55 (6): 679–94.e11. doi: 10.1016/j.devcel.2020.10.015
55. Ayad NME, Almsoud A, Lakins JN, Ghagre A, Ehrlicher AJ, Klein OD, et al. Tissue tension permits β-catenin phosphorylation to drive mesoderm specification in human embryonic stem cells. Dev Cell. 2026; 61 (8): 1652–66.e7. doi: 10.1016/j.devcel.2026.06.014
56. Hennessy MJ, Fulton T, Turner DA, Steventon B. Negative feedback on retinoic acid by Brachyury guides gastruloid symmetry-breaking. bioRxiv. 2023. doi: 10.1101/2023.06.02.543388
57. Mantziou V, Baillie-Benson P, Jaklin M, Kustermann S, Arias AM, Moris N. In vitro teratogenicity testing using a 3D, embryo-like gastruloid system. Reprod Toxicol. 2021; 105: 72–90. doi: 10.1016/j.reprotox.2021.08.003
58. Kim S, Wysocka J. Deciphering the multi-scale, quantitative cis-regulatory code. Mol Cell. 2023; 83 (3): 373–92. doi: 10.1016/j.molcel.2022.12.032
59. Arnold SJ, Stappert J, Bauer A, Kispert A, Herrmann BG, Kemler R. Brachyury is a target gene of the Wnt/β-catenin signaling pathway. Mech Dev. 2000; 91 (1–2): 249–58. doi: 10.1016/s0925-4773(99)00309-3

60. Dahle Ø, Kumar A, Kuehn MR. Nodal signaling recruits the histone demethylase Jmjd3 to counteract polycomb-mediated repression at target genes. Sci Signal. 2010; 3 (127): ra48. doi: 10.1126/scisignal.2000841
61. Chu S, Bell AJ, Lotay V, Ly N, Pells TJ, Kwon T, et al. Xenbase: 25 years of integrating molecular and biomedical data from Xenopus. Genetics. 2026; 232 (4): iyaf237. doi: 10.1093/genetics/iyaf237
62. Casper J, Speir ML, Raney BJ, Perez G, Nassar LR, Lee CM, et al. The UCSC Genome Browser database: 2026 update. Nucleic Acids Res. 2026; 54 (D1): D1331–5. doi: 10.1093/nar/gkaf1250
63. Hinrichs AS, Karolchik D, Baertsch R, Barber GP, Bejerano G, Clawson H, et al. The UCSC Genome Browser Database: update 2006. Nucleic Acids Res. 2006; 34 (Suppl 1): D590–8. doi: 10.1093/nar/gkj144
64. Kemmler CL, Smolikova J, Moran HR, Mannion BJ, Knapp D, Lim F, et al. Conserved enhancers control notochord expression of vertebrate Brachyury. Nat Commun. 2023; 14 (1): 6594. doi: 10.1038/s41467-023-42151-3
65. Faial T, Bernardo AS, Mendjan S, Diamanti E, Ortmann D, Gentsch GE, et al. Brachyury and SMAD signalling collaboratively orchestrate distinct mesoderm and endoderm gene regulatory networks in differentiating human embryonic stem cells. Development. 2015; 142 (12): 2121–35. doi: 10.1242/dev.117838
66. Schifferl D, Scholze-Wittler M, Villaronga Luque A, Pustet M, Wittler L, Veenvliet JV, et al. Genome-wide identification of notochord enhancers comprising the regulatory landscape of the brachyury locus in mouse. Development. 2023; 150 (22): dev202111. doi: 10.1242/dev.202111
67. Schifferl D, Scholze-Wittler M, Wittler L, Veenvliet JV, Koch F, Herrmann BG. A 37 kb region upstream of brachyury comprising a notochord enhancer is essential for notochord and tail development. Development. 2021; 148 (23): dev200059. doi: 10.1242/dev.200059
68. Beisaw A, Tsaytler P, Koch F, Schmitz SU, Melissari MT, Senft AD, et al. BRACHYURY directs histone acetylation to target loci during mesoderm development. EMBO Rep. 2018; 19 (1): 118–34. doi: 10.15252/embr.201744201
69. Nelson AC, Cutty SJ, Gasiunas SN, Deplae I, Stemple DL, Wardle FC. In vivo regulation of the zebrafish endoderm progenitor niche by T-box transcription factors. Cell Rep. 2017; 19 (13): 2782–95. doi: 10.1016/j.celrep.2017.06.011
70. Ye Z, Braden CR, Wills A, Kimelman D. Identification of in vivo Hox13-binding sites reveals an essential locus controlling zebrafish brachyury expression. Development. 2021; 148 (11): dev199408. doi: 10.1242/dev.199408
71. Lerchner W, Latinkic BV, Remacle JE, Huylebroeck D, Smith JC. Region-specific activation of the Xenopus Brachyury promoter involves active repression in ectoderm and endoderm: a study using transgenic frog embryos. Development. 2000; 127 (12): 2729–39. doi: 10.1242/dev.127.12.2729
72. Remacle JE, Kraft H, Lerchner W, Wuytens G, Collart C, Verschueren K, et al. New mode of DNA binding of multi-zinc finger transcription factors: δEF1 family members bind with two hands to two target sites. EMBO J. 1999; 18 (18): 5073–84. doi: 10.1093/emboj/18.18.5073
73. Gentsch GE, Owens NDL, Martin SR, Piccinelli P, Faial T, Trotter MWB, et al. In vivo T-box transcription factor profiling reveals joint regulation of embryonic neuromesodermal bipotency. Cell Rep. 2013; 4 (6): 1185–96. doi: 10.1016/j.celrep.2013.08.012
74. Frank S, Ahuja G, Bartsch D, Russ N, Yao W, Kuo JCC, et al. yylncT defines a class of divergently transcribed lncRNAs and safeguards the T-mediated mesodermal commitment of human PSCs. Cell Stem Cell. 2019; 24 (2): 318–27.e8. doi: 10.1016/j.stem.2018.11.005
75. Hu Y, Mintz A, Shah SR, Quinones-Hinojosa A, Hsu W. The FGFR/MEK/ERK/brachyury pathway is critical for chordoma cell growth and survival. Carcinogenesis. 2014; 35 (7): 1491–9. doi: 10.1093/carcin/bgu014
76. Hu Y, Feng X, Mintz A, Petty WJ, Hsu W. Regulation of brachyury by fibroblast growth factor receptor 1 in lung cancer. Oncotarget. 2016; 7 (52): 87124–35. doi: 10.18632/oncotarget.13547

77. Hu Y, Lu Y, Xing F, Hsu W. FGFR1/MAPK-directed brachyury activation drives PD-L1-mediated immune evasion to promote lung cancer progression. Cancer Lett. 2022; 547: 215867. doi: 10.1016/j.canlet.2022.215867
78. Otani R, Mukasa A, Shin M, Omata M, Takayanagi S, Tanaka S, et al. Brachyury gene copy number gain and activation of the PI3K/Akt pathway: association with upregulation of oncogenic Brachyury expression in skull base chordoma. J Neurosurg. 2018; 128 (5): 1428–37. doi: 10.3171/2016.12.JNS161444
79. Larocca C, Cohen JR, Fernando RI, Huang B, Hamilton DH, Palena C. An autocrine loop between TGF-β1 and the transcription factor brachyury controls the transition of human carcinoma cells into a mesenchymal phenotype. Mol Cancer Ther. 2013; 12 (9): 1805–15. doi: 10.1158/1535-7163.MCT-12-1007
80. Şişli HB, Hayal TB, Şenkal S, Bulut E, Kıratlı B, Asutay AB, et al. Activation of Wnt pathway suppresses growth of MUG-Chor1 chordoma cell line. Cell Biochem Biophys. 2023; 81 (4): 823–37. doi: 10.1007/s12013-023-01178-5
81. Yan X, Li Z, Li H, Liu P, Zhao Z, Cheng S, et al. Inhibition of glycogen synthase kinase 3 beta suppresses the growth and survival of skull base chordoma cells by downregulating Brachyury expression. OncoTargets Ther. 2019; 12: 9783–91. doi: 10.2147/OTT.S218930
82. Sarkar D, Shields B, Davies ML, Müller J, Wakeman JA. BRACHYURY confers cancer stem cell characteristics on colorectal cancer cells. Int J Cancer. 2012; 130 (2): 328–37. doi: 10.1002/ijc.26029
83. Pinto F, Costa ÂM, Andrade RP, Reis RM. Brachyury is associated with glioma differentiation and response to temozolomide. Neurotherapeutics. 2020; 17 (4): 2015–27. doi: 10.1007/s13311-020-00911-9
84. Magnaghi P, Salom B, Cozzi L, Amboldi N, Ballinari D, Tamborini E, et al. Afatinib is a new therapeutic approach in chordoma with a unique ability to target EGFR and Brachyury. Mol Cancer Ther. 2018; 17 (3): 603–13. doi: 10.1158/1535-7163.MCT-17-0324
85. Roselli M, Fernando RI, Guadagni F, Spila A, Alessandroni J, Palmirotta R, et al. Brachyury, a driver of the epithelial-mesenchymal transition, is overexpressed in human lung tumors: an opportunity for novel interventions against lung cancer. Clin Cancer Res. 2012; 18 (14): 3868–79. doi: 10.1158/1078-0432.CCR-11-3211
86. Shao C, Zhang J, Fu J, Ling F. The potential role of Brachyury in inducing epithelial-to-mesenchymal transition (EMT) and HIF-1α expression in breast cancer cells. Biochem Biophys Res Commun. 2015; 467 (4): 1083–9. doi: 10.1016/j.bbrc.2015.09.076
87. Shalaby AAE, Presneau N, Idowu BD, Thompson L, Briggs TRW, Tirabosco R, et al. Analysis of the fibroblastic growth factor receptor-RAS/RAF/MEK/ERK-ETS2/brachyury signalling pathway in chordomas. Mod Pathol. 2009; 22 (8): 996–1005. doi: 10.1038/modpathol.2009.63
88. Yaa RM, Schilder BM, Acemel RD, Wardle FC. Chromatin interaction and histone mark signatures associated with TBXT expression in metastatic lung cancer. Genes Chromosomes Cancer. 2025; 64 (3): e70041. doi: 10.1002/gcc.70041
89. Baranasic D, Hörtenhuber M, Balwierz PJ, Zehnder T, Mukarram AK, Nepal C, et al. Multiomic atlas with functional stratification and developmental dynamics of zebrafish cis-regulatory elements. Nat Genet. 2022; 54 (7): 1037–50. doi: 10.1038/s41588-022-01089-w
90. Robinson JT, Thorvaldsdóttir H, Winckler W, Guttman M, Lander ES, Getz G, et al. Integrative genomics viewer. Nat Biotechnol. 2011; 29 (1): 24–6. doi: 10.1038/nbt.1754
91. Franco HL, Nagari A, Malladi VS, Li W, Xi Y, Richardson D, et al. Enhancer transcription reveals subtype-specific gene expression programs controlling breast cancer pathogenesis. Genome Res. 2018; 28 (2): 159–70. doi: 10.1101/gr.226019.117
92. Kim HJ, Moon SJ, Hong S, Won HH, Kim JH. DBC1 is a key positive regulator of enhancer epigenomic writers KMT2D and p300. Nucleic Acids Res. 2022; 50 (14): 7873–88. doi: 10.1093/nar/gkac585

93. McCleland ML, Mesh K, Lorenzana E, Chopra VS, Segal E, Watanabe C, et al. CCAT1 is an enhancer-templated RNA that predicts BET sensitivity in colorectal cancer. J Clin Investig. 2016; 126 (2): 639–52. doi: 10.1172/JCI83265
94. Gopi LK, Kidder BL. Integrative pan cancer analysis reveals epigenomic variation in cancer type and cell specific chromatin domains. Nat Commun. 2021; 12 (1): 1419. doi: 10.1038/s41467-021-21707-1
95. Nelson AC, Pillay N, Henderson S, Presneau N, Tirabosco R, Halai D, et al. An integrated functional genomics approach identifies the regulatory network directed by brachyury (T) in chordoma. J Pathol. 2012; 228 (3): 274–85. doi: 10.1002/path.4082
96. Cottone L, Cribbs AP, Khandelwal G, Wells G, Ligammari L, Philpott M, et al. Inhibition of histone H3K27 demethylases inactivates Brachyury (TBXT) and promotes chordoma cell death. Cancer Res. 2020; 80 (20): 4540–51. doi: 10.1158/0008-5472.CAN-20-1387
97. Wei J, Wu J, Yin Z, Li X, Liu Y, Wang Y, et al. Low expression of H3K27me3 is associated with poor prognosis in conventional chordoma. Front Oncol. 2022; 12: 1048482. doi: 10.3389/fonc.2022.1048482
98. Baluszek S, Kober P, Rusetska N, Wągrodzki M, Mandat T, Kunicki J, et al. DNA methylation, combined with RNA sequencing, provide novel insight into molecular classification of chordomas and their microenvironment. Acta Neuropathol Commun. 2023; 11 (1): 113. doi: 10.1186/s40478-023-01610-0
99. Wang D, Ding L, Wang L, Zhao Y, Sun Z, Karnes RJ, et al. LncRNA MALAT1 enhances oncogenic activities of EZH2 in castration-resistant prostate cancer. Oncotarget. 2015; 6 (38): 41045–55. doi: 10.18632/oncotarget.5728
100. Fu S, Wang Y, Li H, Chen L, Liu Q. Regulatory networks of lncRNA MALAT-1 in cancer. Cancer Manag Res. 2020; 12: 10181–98. doi: 10.2147/CMAR.S276022
101. Poramba-Liyanage DW, Tong X, Riemers FM, Meij BP, Dilek Y, Cleypool CGJ, et al. Single-cell multi-omics defines H3K27me3 remodelling in intervertebral disc degeneration with implications for regenerative intervention. Bone Res. 2026; 14 (1): 97. doi: 10.1038/s41413-026-00581-x
102. Levental KR, Yu H, Kass L, Lakins JN, Egeblad M, Erler JT, et al. Matrix crosslinking forces tumor progression by enhancing integrin signaling. Cell. 2009; 139 (5): 891–906. doi: 10.1016/j.cell.2009.10.027
103. Le HQ, Ghatak S, Yeung CYC, Tellkamp F, Günschmann C, Dieterich C, et al. Mechanical regulation of transcription controls Polycomb-mediated gene silencing during lineage commitment. Nat Cell Biol. 2016; 18 (8): 864–75. doi: 10.1038/ncb3387
104. Cha TL, Zhou BP, Xia W, Wu Y, Yang CC, Chen CT, et al. Akt-mediated phosphorylation of EZH2 suppresses methylation of lysine 27 in histone H3. Science. 2005; 310 (5746): 306–10. doi: 10.1126/science.1118947
105. Chakraborty AA, Laukka T, Myllykoski M, Ringel AE, Booker MA, Tolstorukov MY, et al. Histone demethylase KDM6A directly senses oxygen to control chromatin and cell fate. Science. 2019; 363 (6432): 1217–22. doi: 10.1126/science.aaw1026
106. Wellen KE, Hatzivassiliou G, Sachdeva UM, Bui TV, Cross JR, Thompson CB. ATP-citrate lyase links cellular metabolism to histone acetylation. Science. 2009; 324 (5930): 1076–80. doi: 10.1126/science.1164097
107. Mentch SJ, Mehrmohamadi M, Huang L, Liu X, Gupta D, Mattocks D, et al. Histone methylation dynamics and gene regulation occur through the sensing of one-carbon metabolism. Cell Metab. 2015; 22 (5): 861–73. doi: 10.1016/j.cmet.2015.08.024